DYNAMICS OF DISCRETE FRAMED STRUCTURES: A UNIFIED HOMOGENIZED DESCRIPTION

Stephane Hans and Claude Boutin

DYNAMICS OF DISCRETE FRAMED STRUCTURES: A UNIFIED HOMOGENIZED DESCRIPTION

STEPHANE HANS AND CLAUDE BOUTIN

The dynamic behavior of discrete periodic one-dimensional structures is approached by considering transverse vibrations of structures made of repeated unbraced frames. Assuming the frame size is small compared to the modal wavelength, equivalent macroscopic beam descriptions are obtained by the homogenization method of periodic discrete media. The macroscopic parameters are expressed as functions of the mechanical and geometrical properties of the frame elements.

Depending on the order of magnitude (relative to the scale ratio) of the shear force, the global bending and the inner bending, four families of beams are shown to be possible. A generic beam governed by a differential equation of the sixth degree is shown to encompass all the other types.

Simple criteria are established to identify the relevant model for real structures. A comparison of these theoretical results with numerical modeling is satisfactory even in the case of weak scale separation. In fact, an investigation of the higher orders terms shows that zero order descriptions are valid up to the second order. Lastly, analogies with micromorphic media are discussed.

1. Introduction

Understanding the behavior of reticulated materials and structures is of interest in aeronautics (lattice beams), in civil engineering (buildings), in materials science (mechanics of foam or glass wool), in biomechanics (vegetable tissue or bones), and so on. When the dimensions of the representative cell are smaller than the overall size, such three-, two-, or one-dimensional systems may be described respectively by effective continuum media, plate or beam models. Numerous studies have been aimed at relating the local structure to the global behavior. Particularly, periodic lattices have been studied through various approaches such as transfer matrices, variational calculus [Kerr and Accorsi 1985], and finite difference operators [Renton 1984]; see also the reviews [Noor 1988; Mead 1996]. Asymptotic homogenization methods [Sánchez-Palencia 1980] have been developed for homogeneous and periodic beams [Trabucho and Viaño 1996; Buannic and Cartraud 2001a; 2001b], for periodic discrete structures [Bakhvalov and Panasenko 1989; Caillerie et al. 1989], and in parallel with the homogenization of periodic media with multiple parameters and scale changes [Cioranescu and Saint Jean Paulin 1999]. Amongst the applications of homogenization of periodic discrete media (HPDM) we mention the papers [Tollenaere 1994; Moreau and Caillerie 1998; Boutin and Hans 2003], dealing respectively with the statics, buckling and dynamics of trusses; [Pradel and Sab 1998], on the constitutive laws of foams; and [Le Corre et al. 2004], involving fluid mechanics.

The present study, initially motivated by earthquake engineering, is concerned with the dynamics of framed beams, which may be seen as "idealized buildings". Among the numerous possible basic

cell architectures of one-dimensional repetitive structures, HPDM investigation of an orthogonal grid geometry is of interest for the following reasons:

– The lack of bracing means that cells have a much lower shear stiffness than compression stiffness. In this case, which is not uncommon in structural engineering, the method of multiple parameters and scale changes [Cioranescu and Saint Jean Paulin 1999] captures the leading order (compression) but misses the shear properties, which are found to vanish (with a loss of convexity of the elastic potential), whereas in fact they are of lower order. HPDM overcomes this bias and predicts behaviors that are not derivable by more classical upscaling methods. See [Buannic and Cartraud 2001a; 2001b], for example.

– It will be shown that the diversity of beam-like behaviors of repetitive structures [Stephen 1999] is recovered by varying the mechanical properties of the basic frame elements. The high contrast of shear and compression deformability enriches the local kinematics, inducing new beam-like models. The macro behaviors can be classified according to three intrinsic mechanical parameters characterizing the cell. Since these global parameters can be derived for any cell (braced or not), framed beams can be considered as an archetypical case and the results extended to other kind of reticulated beams.

– The strength of HPDM is to derive, without any prerequisite other than scale separation, a rigorous and analytical continuous beam-like description in direct relation with the characteristics of the cell elements. The formulation enables a parametric study and provides a clear understanding of the several mechanisms governing the global behavior. The continuous description also highlights and simplifies the modal analysis of the structure. This global vision is not accessible through finite element modeling, which gives accurate numerical descriptions attached to a particular structure.

A first investigation on this topic was initiated in [Boutin and Hans 2003]. The wider objectives of the present work are:

– To work out all possible transverse dynamic behaviors of these structures and to define in each case the equivalent beam modeling. Depending on the mechanical properties of the cell, four families of beams are identified. A *generic beam*, governed by a differential equation of sixth degree, is proved to include all other mechanisms. This macro beam modeling involves three kinematic variables, namely section translation, rotation and inner deformation dual to shear force, bending and inner moments.

– To provide criteria to identify which model is relevant to a given real structure and to analyze the range of validity and the accuracy of the continuum modeling. It is demonstrated that *the maximum number of homogenizable modes is of the order of a third of the number of cells*. By investigating correctors of higher orders, the zero order description is shown to be correct up to second order. This may explain the fairly good accuracy of the continuum beam method that is observed numerically.

– To point out the analogy between these descriptions and those of micromorphic materials such as Cosserat media or inner deformation media. Using a dimensional analysis based on the intrinsic parameters of the cell, the conditions under which a reticulated medium may behave as a generalized medium at the zero order are presented and discussed.

The principles of the method will be given in Section 2 and applied to framed structures in Section 3. The beam models are presented in Section 4. Their applications and numerical validation are discussed in Section 5. Analogies with micromorphic media are developed in Section 6. The detailed implementation of HPDM for framed structures is reported in Section 7.

2. The method of homogenization of discrete periodic media (HDPM)

The modal analysis of periodic lattices of interconnected beams is performed by HDPM in two steps [Tollenaere and Caillerie 1998]: discretization of the balance of the structure under harmonic vibrations, followed by the homogenization, leading to a continuous model obtained from the discrete description. An outline of this method is given now; a detailed exposition including an example is given in Section 7.

Discretization of the dynamic balance. The structures we consider (see Figure 1 on page 1713) are made of plate behaving as pure Euler-Bernoulli beam in out-of-plane motion. They are assembled with perfectly stiff connections. Thus, the motions of each endpoint connected to the same node are identical and define the discrete nodal kinematic variables of the system. The discretization consists in integrating the dynamic balance (in harmonic regime) of the beams, the unknown displacements and rotations at their endpoints being taken as boundary conditions. Forces applied by an element on its endpoints are then expressed explicitly as functions of the nodal kinematic variables; see (7-7). The dynamic balance of each element being satisfied, it remains to express the balance of forces applied by the elements connected to a same node. Thus, the balance of the whole structure is rigorously reduced to the balance of the set of nodes; that is, the discrete description using only the nodal variables is fully equivalent to the complete description.

Asymptotic expansions. The key assumption of HPDM is scale separation. This means that the cell size ℓ (in the direction of the periodicity) is small compared to the unknown characteristic size L of the deformation of the structure under vibrations. Thus the scale ratio $\varepsilon = \ell/L$ is such that $\varepsilon \ll 1$. The existence of a macroscale implies that HDPM is limited to low frequency modes whose wavelength is large compared to the cell size. In this case, the forces and displacements vary slowly from one node to the next and can be considered as the discrete values of continuous functions to be determined. For this purpose, a macroscopic space variable x is introduced along the periodicity axis and variables are expressed as continuous functions of x coinciding with the discrete variable at any node n ($x = x_n$). For instance, a continuous displacement $U_\varepsilon(x)$ is defined in such a way that

$$U_\varepsilon(x = x_n) = U(\text{node } n).$$

These quantities, assumed to converge when ε tends to zero, are expanded in powers of ε. This introduces the continuous functions U^i of order i:

$$U_\varepsilon(x) = U^0(x) + \varepsilon\, U^1(x) + \varepsilon^2\, U^2(x) + \cdots. \tag{2-1}$$

Later on, the physically observable variables of a given order in ε will be denoted by a tilde; for example,

$$\tilde{U}^i(x) = \varepsilon^i U^i(x).$$

All unknowns, including the modal frequency, will be expanded in powers of ε.

Since $\ell = \varepsilon L$ is small with respect to x, the variation in variables between neighboring nodes $n-1$ and $n+1$ is expressible using Taylor series; this in turn leads to the macroscopic derivatives. For instance,

$$U(n \pm 1) = U^0(x_n) + \varepsilon\big(U^1(x_n) \pm L\, U^{0'}(x_n)\big) + \varepsilon^2\big(U^2(x_n) \pm L\, U^{1'}(x_n) + \tfrac{1}{2}L^2\, U^{0''}(x_n)\big) + \cdots$$

Here, the periodicity is explicitly used and the constant internodal distance enables one to express these Taylor expansions with a single parameter ε. Finally, scale separation requires that, at the modal frequency of the global system, the wavelength generated in each local element be much longer than the element's length. Consequently, nodal forces can be developed in Taylor series with respect to ε (expressions are given in Section 7D).

Normalization. To account properly for the local physics, it is necessary to integrate correctly the properties of the cell through a normalization. Indeed, the method of asymptotic expansions is based on the identification of terms of the same power of ε in the expansions of the balance equations. The identification makes sense under the condition that ε tends to 0.

The normalization consists in scaling the geometric and mechanical characteristics of the element according to the powers of ε. As for the modal frequency, scaling is imposed by the balance of elastic and inertia forces at the macro level. Such a normalization insures that each mechanical effect appears at the same order whatever the value of ε. Therefore, the same physics is kept at the limit $\varepsilon \to 0$, which represents the homogenized model.

Macroscopic description. Expansions in powers of ε are introduced in the nodal balances. The relations obtained being valid for any small enough ε, the orders can be separated. This leads to balance equations for each order, whose resolution defines the macroscopic governing equations. The descriptions presented in Section 4 are limited to the leading order. Correctors of interest in the case of poor scale separation are examined in Section 5.

3. Class of structures

Our study focuses on the harmonic transverse vibrations in the plane (e_1, e_2) of structures constituted by a pile of a large number N of identical unbraced frames called cells (Figure 1). Cell elements, of length h in the direction e_3, are linked by stiff massless connections and behave as Euler-Bernoulli beams. The following notation will be used:

- Level n contains two nodes, n_1 on the left and n_2 on the right. Cell n is made of one horizontal element fn (the floor) of level n, supported by two vertical elements wn_1 and wn_2 (walls) linking level $n-1$ and level n.

- The parameters of walls ($i = w$) and floors ($i = f$) are: length ℓ_i; thickness a_i; section area A_i; inertia in direction e_3 $I_i = a_i^3 h/12$; density ρ_i; elastic modulus E_i (Young's modulus E_Y in the case of beam or $E_Y/(1-\nu)$ in the case of plates as considered here). The height of the structure is $H = N\ell_w$.

Local variables. At level n, the motion of node n_i ($i = 1, 2$) in the plane (e_1, e_2) is described by the displacements $u_1(n_i)$, $u_2(n_i)$ in the two directions and by the rotation $\theta(n_i)$. Because of longitudinal symmetry, these six variables can be replaced by the three variables $(U(n), \alpha(n), V(n))$ associated to the
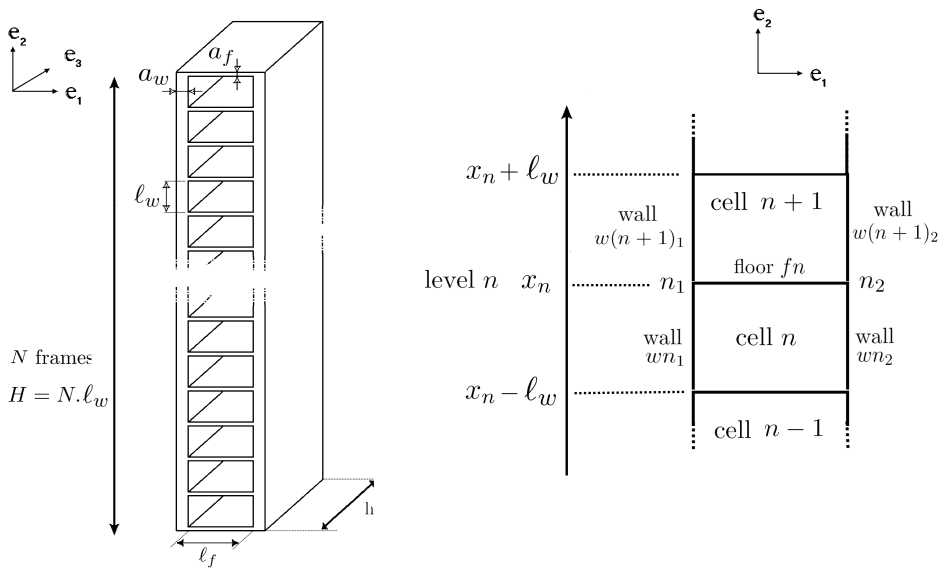
Figure 1. The class of unbraced framed structures studied in this paper (left) and the basic frame and notations (right).

rigid body motion of the pair of nodes (n_1, n_2) and the three variables $(\theta(n), \Delta(n), \Phi(n))$ corresponding to the deformation of (n_1, n_2); see Figure 2. The expressions of the variables are

$$\begin{cases} U(n) &= (u_1(n_1) + u_1(n_2))/2 & \text{Mean transverse displacement (along } e_1) \\ \alpha(n) &= (u_2(n_1) - u_2(n_2))/\ell_f & \text{Rotation of level } n \\ \theta(n) &= (\theta(n_1) + \theta(n_2))/2 & \text{Mean rotation of nodes} \end{cases}$$

$$\begin{cases} V(n) &= (u_2(n_1) + u_2(n_2))/2 & \text{Mean axial displacement (along } e_2) \\ \Delta(n) &= u_1(n_2) - u_1(n_1) & \text{Transverse dilatation} \\ \Phi(n) &= \theta(n_2) - \theta(n_1) & \text{Differential rotation of nodes} \end{cases}$$

At level n, the action of cell n on cell $n+1$ consists in the transverse and longitudinal forces $\text{T}(n_i)$ and $\text{N}(n_i)$, and the moments $\text{M}(n_i)$, $i = 1, 2$. These forces are exactly the opposite of those in the two walls of cell $n+1$ at the connections with cell n. It is convenient to introduce the total and differential
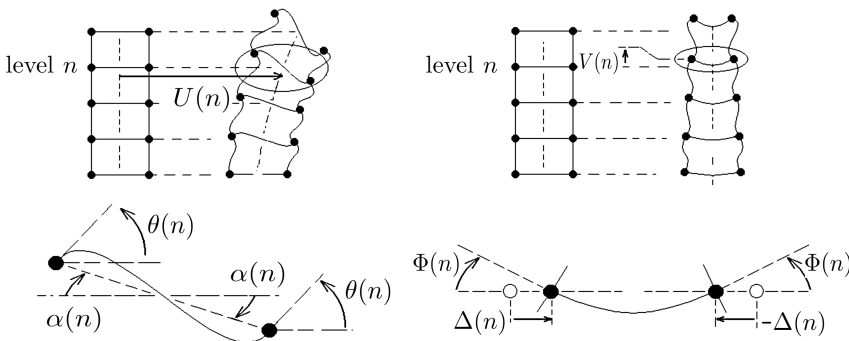
Figure 2. Decoupling of transverse (left) and longitudinal (right) kinematics.

forces defined by

$$
\begin{cases}
\text{T}_t(n) &= \text{T}(n_1) + \text{T}(n_2) & \text{Total transverse force} \\
\text{M}(n) &= \ell_f(\text{N}(n_2) - \text{N}(n_1)) & \text{Moment of the differential longitudinal force} \\
\text{M}_t(n) &= \text{M}(n_1) + \text{M}(n_2) & \text{Total inner moment}
\end{cases}
$$

$$
\begin{cases}
\text{N}_t(n) &= \text{N}(n_1) + \text{N}(n_2) & \text{Total longitudinal force} \\
\text{T}_d(n) &= \text{T}(n_2) - \text{T}(n_1) & \text{Differential transverse force} \\
\text{M}_d(n) &= \text{M}(n_2) - \text{M}(n_1) & \text{Differential inner moment}
\end{cases}
$$

There are six nodal balance equations, derived in Section 7 as (7-8), (7-9):

Node n_1: $\text{T}^E_{wn_1} - \text{T}^B_{w(n+1)_1} - \text{N}^B_{fn} = 0$, $\text{N}^E_{wn_1} - \text{N}^B_{w(n+1)_1} - \text{T}^B_{fn} = 0$, $\text{M}^E_{wn_1} - \text{M}^B_{w(n+1)_1} - \text{M}^B_{fn} = 0$, (3-1)

Node n_2: $\text{T}^E_{wn_2} - \text{T}^B_{w(n+1)_2} + \text{N}^E_{fn} = 0$, $\text{N}^E_{wn_2} - \text{N}^B_{w(n+1)_2} + \text{T}^E_{fn} = 0$, $\text{M}^E_{wn_2} - \text{M}^B_{w(n+1)_2} + \text{M}^E_{fn} = 0$, (3-2)

Longitudinal symmetry enables to split them into two uncoupled sets of three equations, governing independently the transverse and longitudinal vibrations. Transverse vibrations are described by $U(n)$, $\theta(n)$ and $\alpha(n)$ involved in the following balance equations associated with the forces $\text{T}_t(n)$, $\text{M}_t(n)$ and $\text{M}(n)$:

$$
\text{Balance of} \begin{cases}
\text{T}_t(n) & \text{given by } (3\text{-}1)_1 + (3\text{-}2)_1 \\
\text{M}(n) & \text{given by } (3\text{-}2)_2 - (3\text{-}1)_2 \\
\text{M}_t(n) & \text{given by } (3\text{-}2)_3 + (3\text{-}1)_3
\end{cases}
\tag{3-3}
$$

We will focus on transverse vibrations, but longitudinal vibrations, described by the complementary set (namely $(3\text{-}1)_1 + (3\text{-}2)_1$, $(3\text{-}2)_2 - (3\text{-}1)_2$, $(3\text{-}2)_3 - (3\text{-}1)_3$) and involving $V(n)$, $\Delta(n)$ and $\Phi(n)$ and the forces $\text{N}_t(n)$, $\text{T}_d(n)$ and $\text{M}_d(n)$, can be analyzed in the same manner [Boutin and Hans 2003].

Scaling. We consider structures whose walls and floors have similar lengths and are made of elastic linear materials with moduli and densities of the same order of magnitude:

$$
E_f/E_w = O(1), \qquad \rho_f/\rho_w = O(1), \qquad \ell_f/\ell_w = O(1).
$$

The various physics of the basic frame are introduced through the walls and floors thicknesses that may be different, hence inducing a large range of contrast of stiffness between elements, in compression and bending. Those properties are specified by scaling the wall and floor thicknesses:

$$
a_w/\ell_w = O(\varepsilon^{k_w}) \text{ and } a_f/\ell_w = O(\varepsilon^{k_f}),
$$

where k_w and k_f are fixed for each investigated structure. The reference frequency used for scaling the modal frequencies is taken by convention as

$$
\omega_r = \frac{1}{L}\sqrt{\frac{2\,E_w A_w}{\Lambda}},
\tag{3-4}
$$

where Λ is the global linear mass of the structure. The modal frequency is scaled through the ratio of the length of elements to their wavelength at this frequency. Because of linearity, the modes can be normalized and the mean transverse displacement order is chosen at zero. The effective orders of magnitude with respect to U^0/L of the rotation of the section α and of the mean nodal rotation θ, are deduced through the homogenization process.

Macroscopic parameters. In the expansions there appear naturally

(a) the linear masses of
$$\begin{cases} \text{the two walls,} & \Lambda_w = 2\rho_w A_w, \\ \text{the floor,} & \Lambda_f = \rho_f A_f \ell_f / \ell_w, \\ \text{the cell,} & \Lambda = \Lambda_f + \Lambda_w; \end{cases}$$

(b) the bending stiffnesses of the two walls,
$$\begin{cases} \text{(inner bending)} & 2E_w I_w, \quad \text{where } I_w = a_w^3 h/12, \\ \text{(global bending)} & E_w I = E_w A_w \ell_f^2/2; \end{cases}$$

(c) the macroscopic shear stiffnesses of
$$\begin{cases} \text{the two walls,} & K_w = 2\kappa_w \ell_w, \quad \text{where } \kappa_w = 12E_w I_w/\ell_w^3, \\ \text{the floor,} & K_f = \kappa_f \ell_f^2/\ell_w, \quad \text{where } \kappa_f = 12E_f I_f/\ell_f^3, \\ \text{the cell,} & K^{-1} = K_w^{-1} + K_f^{-1}. \end{cases}$$

The macroscopic area moment of inertia I is that of a beam made of the two walls distant of ℓ_f, and $\kappa_i = 12E_i I_i/\ell_i^3$ is the static bending stiffness of a bi-embedded beam.

4. Transverse dynamics of multi-framed structures

This section shows that the structures considered can exhibit four main kinds of behavior, according to the frame characteristics. Starting from the three discrete kinematic variables $U(n)$, $\alpha(n)$ and $\theta(n)$, the beam-like model can be governed either

- by the single continuous variable U, corresponding to a *shear beam*,

- or by the two independent continuous variables U and α, corresponding to a *slender-Timoshenko beam*,

- or by U and θ, corresponding to an *inner bending / shear beam*,

- or by the three independent continuous variables U, α and θ when transferred to a macroscopic scale, in which case a *double bending shear beam* is obtained.

These models can be considered as particular cases of a *generic beam*.

Shear beam. The simplest macroscopic description is obtained (for instance) when walls and floors have thicknesses of order ε^2: in symbols, $a_w/\ell_w = O(\varepsilon^2)$ and $a_f/\ell_w = O(\varepsilon^2)$.

Leading macroscopic balance equations. In this case, the macroscopic transverse dynamics occurs at frequency ω of order $O(\omega_r(a_w/\ell_w)) = O(\omega_r\varepsilon^2)$, denoted for this reason $\tilde{\omega}_2$. The variables $\tilde{U}^0$ and $\tilde{\theta}^0$ are of the zero order, while the section rotation $\tilde{\alpha}^2$ is of the second order. Considered to leading order, Equations (3-3) give

$$\begin{cases} K_w(\tilde{U}^{0''} + \tilde{\theta}^{0'}) + \Lambda\tilde{\omega}_2^2 \tilde{U}^0 = 0 & (\text{T}_t) \\ K_w(\tilde{U}^{0'} + \tilde{\theta}^0) + K_f \tilde{\theta}^0 = 0 & (\text{M}_t) \\ K_f\tilde{\theta}^0 + E_w I\tilde{\alpha}^{2''} = 0 & (\text{M}) \end{cases} \tag{4-1}$$

These equations represent the balance of, respectively, transverse forces, inner moments and differential axial forces (inducing a macroscopic moment). The relation (4-1)M_t defines the inner kinematic of the section. Using this relation for eliminating $\tilde{\theta}^0$ in (4-1)T_t, we obtain a differential equation of second degree in $\tilde{U}^0$:

$$K\tilde{U}^{0''} + \Lambda\tilde{\omega}_2^2 \tilde{U}^0 = 0. \tag{4-2}$$

Thus, $\tilde{U}^0$ appears as the single driving macroscopic variable. The inner deformation of the section measured by $\tilde{\theta}^0$ and the rotation $\tilde{\alpha}^2$ can be derived from the knowledge of $\tilde{U}^0$ by means of the equations

$$\tilde{\theta}^0 = -\frac{K}{K_f}\tilde{U}^{0'}, \qquad \tilde{\alpha}^{2''} = \frac{K}{E_w I}\tilde{U}^{0'}. \tag{4-3}$$

Equivalent beam. These results allow one to construct an equivalent beam by defining the appropriate behavior law. Equation (4-2) suggests that we define a macroscopic shear force $\tilde{T}^0$ dual to the section translation $\tilde{U}^0$ whose variations balance the inertia:

$$\tilde{U}^{0'} = \Lambda \tilde{\omega}_2^2 \, \tilde{U}^0. \tag{4-4}$$

This gives

$$\tilde{T}^0 = -K \, \tilde{U}^{0'}. \tag{4-5}$$

The force $\tilde{T}^0$ results from the balance of transverse force T_t, but they are not identical; the former is built from the elastic deformation (of the first order) exclusively, whereas T_t contains all the effects, including the inertia. Equations (4-4) and (4-5) correspond to the macroscopic shear beam equivalent to (4-2) and governed by the two dual variables, $\tilde{U}^0$ and $\tilde{T}^0$ that are sufficient to define the proper boundary conditions for transverse vibrations. The macroscopic shear force is generated by the shear mechanism of the frame. This latter results from the bending of frames beams bi-embedded at their endpoints, as suggested by physical intuition and confirmed by the expression of K (item (c) on page 1715). The shear beam reduces the three degrees of freedom at the local scale to one - the section translation - at the macro scale. Although $\tilde{\theta}^0$ is of the zero order, it disappears, as $\tilde{\alpha}^2$, in the macro description. These last variables have the status of "hidden" internal variables driven by the macro variable, as indicated in (4-3). This shear beam is the continuous version of the shear model widely used in earthquake engineering.

Slender-Timoshenko beam. Consider now structures whose wall and floor thicknesses are of the same order as the scale ratio, so $a_w/\ell_w = O(\varepsilon)$ and $a_f/\ell_w = O(\varepsilon)$.

Leading macroscopic balance equations. In this case, detailed in Section 7F, transverse vibrations occur at frequency $\tilde{\omega}_1$ of order $O(\omega_r(a_w/\ell_w)) = O(\omega_r\varepsilon)$ and variables $\tilde{U}^0$, $\tilde{\theta}^0$, $\tilde{\alpha}^0$ are of the zero order. Considered to leading order, Equations (3-3) yield

$$\begin{cases} K_w\big(\tilde{U}^{0''} + \tilde{\theta}^{0'}\big) + \Lambda\tilde{\omega}_1^2\,\tilde{U}^0 = 0 & (T_t) \\ K_w\big(\tilde{U}^{0'} + \tilde{\theta}^0\big) + K_f\big(\tilde{\theta}^0 - \tilde{\alpha}^0\big) = 0 & (M_t) \\ K_f\big(\tilde{\theta}^0 - \tilde{\alpha}^0\big) + E_w I\tilde{\alpha}^{0''} = 0 & (M) \end{cases} \tag{4-6}$$

As above, the balance of inner moments (4-6)M_t provides the inner kinematic of the section,

$$\tilde{\theta}^0 = K\left(\frac{\tilde{\alpha}^0}{K_w} - \frac{\tilde{U}^{0'}}{K_f}\right). \tag{4-7}$$

The use of this relation to eliminate $\tilde{\theta}^0$ in (4-6)T_t and (4-6)M gives

$$\begin{cases} K\big(\tilde{U}^{0''} + \tilde{\alpha}^{0'}\big) + \Lambda\tilde{\omega}_1^2\tilde{U}^0 = 0, \\ K\big(\tilde{U}^{0'} + \tilde{\alpha}^0\big) - E_w I\tilde{\alpha}^{0''} = 0. \end{cases} \tag{4-8}$$

This shows that the translation $\tilde{U}^0$ and the rotation $\tilde{\alpha}^0$ of the section are the two independent governing variables, while $\tilde{\theta}^0$ is linked to them by (4-7). Combining the two parts of (4-8) we obtain

$$E_w I \left(\tilde{U}^{0''''} + \frac{\Lambda \tilde{\omega}_1^2}{K} \tilde{U}^{0''} \right) - \Lambda \tilde{\omega}_1^2 \tilde{U}^0 = 0 \qquad (4\text{-}9)$$

Equivalent beam. The preceding description is close to that of a Timoshenko beam. The presence of two kinematic variables leads us to introduce a shear force $\tilde{T}^0$ dual to the translation and a bending moment $\tilde{M}^0$ dual to the section rotation. From (4-8), they are defined by

$$\tilde{T}^0 = -K \left(\tilde{U}^{0'} + \tilde{\alpha}^0 \right), \qquad \tilde{M}^0 = E_w I \, \tilde{\alpha}^{0'}, \qquad (4\text{-}10)$$

so that the macro description (4-8) is now

$$\tilde{T}^{0'} = \Lambda \tilde{\omega}_1^2 \tilde{U}^0, \qquad \tilde{M}^{0'} = -\tilde{T}^0 \qquad (4\text{-}11)$$

meaning that the variations of shear force balance the inertial effect, and those of bending moment balance the shear force (as in classical beam theory). The macroscopic shear force (4-10)$_1$ is generated by the shear deformation of the cell already described for the shear beam. The shear distortion of the cell now combines the gradient of the translation and the section rotation. The macroscopic bending moment of the whole structure comes from simultaneous traction-compression of walls, as indicated by the expression of the macro area moment of inertia I (item (b) on page 1715). The behavior laws (4-10) are those of a beam described by

– the translation $\tilde{U}^0$ and rotation $\tilde{\alpha}^0$ of the section, and
– the shear force $\tilde{T}^0$ and bending moment $\tilde{M}^0$.

which suffice to express the correct macroscopic boundary conditions. The number of degrees of freedom is once again reduced since $\tilde{\theta}^0$ disappears from the macro description to become a "hidden" internal variable defined from the driving variables by (4-7).

Despite similarities, this model does not exactly fit the usual Timoshenko beam for two reasons. First, for massive beams, the Timoshenko correction due to shear only arises in case of small slenderness. Here the shear effect is present even for large slenderness. Secondly, for a Timoshenko massive beam, no effect of rotation inertia appears (although the discrete moment balances include all the contributions). These differences come from the framed cell whose shear deformability is much larger than in a massive beam and whose rotation inertia is much smaller (so its effect appears only at higher orders).

Note on the scaling. We will prove for the case at hand that transverse modes only occur for frequencies $\omega = O(\omega_r(a_w/\ell_w))$ (the arguments apply to other cases as well). At a frequency $\omega \ll \omega_r(a_w/\ell_w)$, the inertia $\Lambda_w \omega^2 \tilde{U}^0$ disappears from (4-6)$_{T_t}$, so a quasistatic solution would be obtained. Conversely, at a frequency $\omega \gg \omega_r(a_w/\ell_w)$, (4-6)$_{T_t}$ reduces to $\Lambda_w \omega^2 \tilde{U}^0 = 0$, so $\tilde{U}^0 = 0$. Thus, we are left with equations involving $\tilde{\alpha}^0$ and $\tilde{\theta}^0$. Such *gyration* deformations without translation at the leading order do not correspond to a transverse mode.

Inner bending / shear beam. A less usual behavior arises when $a_w = O(\varepsilon \ell_w)$ and, say $a_f = O(\varepsilon^{5/3} \ell_w)$: in other words, when the floors are significantly more flexible than the walls, since $K_f = O(\varepsilon^2 K_w)$.

Leading macroscopic balance equations. In this case, transverse vibrations occur for frequencies $\tilde{\omega}_2$ of order $O(\omega_r(a_w/\ell_w)^2)$; $\tilde{U}^0$ and $\tilde{\theta}^0$ are of zero order, and $\tilde{\alpha}^2$ is of second order. The derivation of the behavior requires considering the first two orders of the transverse force and inner moment balances, $(3\text{-}3)_1$ and $(3\text{-}3)_3$, together with the leading order of the bending moment balance $(3\text{-}3)_2$. We obtain

$$
\begin{aligned}
K_w\big(\tilde{U}^{0''} + \tilde{\theta}^{0'}\big) &= 0 &&(\text{T}_t)\\
K_w\big(\tilde{U}^{2''} + \tilde{\theta}^{2'}\big) + \Lambda_w\tilde{\omega}_2^2\tilde{U}^0 + 2E_wI_w\big(\tilde{U}^{0''''} + 2\tilde{\theta}^{0'''}\big) &= 0 &&(\text{T}_{t1})\\
K_w\big(\tilde{U}^{0'} + \tilde{\theta}^0\big) &= 0 &&(\text{M}_t)\\
K_w\big(\tilde{U}^{2'} + \tilde{\theta}^2\big) + K_f\tilde{\theta}^0 \quad + 2E_wI_w\big(2\tilde{U}^{0'''} + 2\tilde{\theta}^{0''}\big) &= 0 &&(\text{M}_{t1})\\
K_f\tilde{\theta}^0 \qquad\qquad + E_wI\tilde{\alpha}^{2''} &= 0 &&(\text{M})
\end{aligned}
\tag{4-12}
$$

As before, the zero order nodal moment balance supplies the inner kinematic of the section:

$$
\tilde{U}^{0'} + \tilde{\theta}^0 = 0 \tag{4-13}
$$

The elimination of the second order terms between $(4\text{-}12)_{\text{T}t1}$ and $(4\text{-}12)_{\text{M}t1}$ leads to

$$
2E_wI_w\,\tilde{U}^{0''''} = K_f\,\tilde{U}^{0''} + \Lambda_w\tilde{\omega}_2^2\,\tilde{U}^0. \tag{4-14}
$$

The behavior (4-14) differs fundamentally from that of the slender-Timoshenko beam. Here, the fourth degree term results from inner bending of walls. The quantity $2E_wI_w$ indicates the coupling between walls, due to the nonlengthening of floors, very stiff in their axis. This coupling enforces the bi-embedded bending of the floors (of very low transverse stiffness K_f), which in turn induces a transverse force. Equations (4-14) and (4-13) imply that the driving variables are the translation $\tilde{U}^0$ and the inner deformation of the section expressed by $\tilde{\theta}^0$. The section rotation, of order two, is a *hidden* internal variable defined by

$$
\tilde{\alpha}^{2''} = \frac{K_f}{E_wI}\,\tilde{U}^{0'}. \tag{4-15}
$$

Equivalent beam. According to these results, two macroscopic forces are defined, a shear force $\tilde{T}^0$ dual to the translation and an inner bending moment $\tilde{\mathcal{M}}^0$ dual to the inner deformation:

$$
\tilde{T}^0 = -K_f\,\tilde{U}^{0'}, \qquad \tilde{\mathcal{M}}^0 = -2E_wI_w\,\tilde{\theta}^{0'}. \tag{4-16}
$$

$\tilde{T}^0$ takes a form similar to that of the previous beams, except that shear stiffness is induced by the floors alone and the section rotation disappears. The inner moment $\tilde{\mathcal{M}}^0$ due to the simultaneous bending of the walls is new. Using these variables, (4-13) and (4-14) become

$$
\big(\tilde{T}^0 + \tilde{\mathcal{M}}^{0'}\big)' = \Lambda\tilde{\omega}_2^2\,\tilde{U}^0, \qquad \tilde{\theta}^0 = -\tilde{U}^{0'}. \tag{4-17}
$$

The first of these equations means that the inertia is balanced by the variation of the total shear force, which includes $\tilde{T}^0$, induced by the shear of the cell, and the shear force $\tilde{\mathcal{M}}^{0'}$, due to the inner bending of the walls. The inner moment balance $(4\text{-}17)_2$ defines the inner kinematic of the section. In accordance with $(4\text{-}12)_{\text{M}}$, a global bending moment $\tilde{M}^0 = E_wI\tilde{\alpha}^{2'}$ such that $\tilde{M}^{0'} = -\tilde{T}^0$ could also be defined, but its effect (traction-compression of walls) is insignificant.

We conclude that the inner bending / shear beam is described by the following macroscopic variables, sufficient to express the macroscopic boundary conditions:

– the section translation $\tilde{U}^0$ and inner deformation associated to the rotation $\tilde{\theta}^0$;
– the shear force $\tilde{T}^0$ and inner bending moment $\tilde{\mathcal{M}}^0$.

This beam model, where the cell inner deformation subsists as a macroscopic variable, is of the same kind as the one proposed by [Kerr and Accorsi 1985].

Double bending shear beam. Here is now investigated the particular situation allowing the global bending, the inner bending of walls and the shear of the cell to have similar intensity. This specific case occurs when $a_w/\ell_w = O(1)$ and $a_f/\ell_w = O(\varepsilon^{2/3})$ so that $K_f = O(\varepsilon^2 K_w)$.

Leading macroscopic balance equations. In this case, the transverse vibrations occur at frequency $\tilde{\omega}_1$ of order $O(\omega_r(a_w/\ell_w))$ and $\tilde{U}^0$, $\tilde{\theta}^0$, $\tilde{\alpha}^0$ are of zero order. As in the previous case, the determination of the behavior requires the first two orders of the mean transverse force and inner moment balances, $(3\text{-}3)_1$ and $(3\text{-}3)_3$, and the leading order of global moment balance $(3\text{-}3)_2$. We obtain

$$
\begin{aligned}
K_w\big(\tilde{U}^{0''} + \tilde{\theta}^{0'}\big) &= 0 \quad (\mathrm{T}_t) \\
K_w\big(\tilde{U}^{2''} + \tilde{\theta}^{2'}\big) \;+\; \Lambda_w\tilde{\omega}_1^2\tilde{U}^0 + 2E_wI_w\big(\tilde{U}^{0''''} + 2\tilde{\theta}^{0'''}\big) &= 0 \quad (\mathrm{T}_{t1}) \\
K_w\big(\tilde{U}^{0'} + \tilde{\theta}^{0}\big) &= 0 \quad (\mathrm{M}_t) \\
K_w\big(\tilde{U}^{2'} + \tilde{\theta}^{2}\big) + K_f\big(\tilde{\theta}^{0} - \tilde{\alpha}^{0}\big) + 2E_wI_w\big(2\tilde{U}^{0'''} + 2\tilde{\theta}^{0''}\big) &= 0 \quad (\mathrm{M}_{t1}) \\
K_f\big(\tilde{\theta}^{0} - \tilde{\alpha}^{0}\big) + E_wI\tilde{\alpha}^{0''} &= 0 \quad (\mathrm{M})
\end{aligned}
\tag{4-18}
$$

This system is similar to that of the inner bending / shear beam, but $\tilde{\alpha}^0$ appears in (4-18)M_{t1} and (4-18)M. Elimination of the second order terms between (4-18)T_{t1} and (4-18)M_{t1} leads to

$$
\tilde{U}^{0'} + \tilde{\theta}^{0} = 0, \quad K_f\big(\tilde{\theta}^{0} - \tilde{\alpha}^{0}\big) - \Lambda_w\tilde{\omega}_1^2\tilde{U}^0 + 2E_wI_w\tilde{U}^{0''''} = 0, \quad K_f\big(\tilde{\theta}^{0} - \tilde{\alpha}^{0}\big) + E_wI\tilde{\alpha}^{0''} = 0. \tag{4-19}
$$

Combining these three equations gives the sixth-degree differential equation

$$
\frac{2E_wI_wE_wI}{K_f}\,\tilde{U}^{0''''''} - \big(2E_wI_w + E_wI\big)\,\tilde{U}^{0''''} - \frac{E_wI\,\Lambda_w\tilde{\omega}_1^2}{K_f}\,\tilde{U}^{0''} + \Lambda_w\tilde{\omega}_1^2\,\tilde{U}^0 = 0. \tag{4-20}
$$

Equation (4-20) shows that this nonclassical beam integrates the three previously identified mechanisms and requires three kinematic variables. Remarkably, the degrees of freedom at the macro scale are identical to those at the micro scale. Consequently, this is the richest continuous modeling that can be extracted from the class of discrete structures under study.

Equivalent beam. The beam-like description involves three forces dual to the section translation $\tilde{U}^0$ and rotation $\tilde{\alpha}^0$, the inner deformation $\tilde{\theta}^0$. They are defined by

$$
\begin{cases}
\text{shear force} & \tilde{T}^0 = -K_f\big(\tilde{U}^{0'} + \tilde{\alpha}^{0}\big) \\
\text{bending moment} & \tilde{M}^0 = E_wI\tilde{\alpha}^{0'} \\
\text{inner moment} & \tilde{\mathcal{M}}^0 = -2E_wI_w\tilde{\theta}^{0'}
\end{cases}
\tag{4-21}
$$

and Equations (4-19) now read

$$(\tilde{T}^0 + \tilde{M}^{0'})' = \Lambda_w \tilde{\omega}_1^2 \tilde{U}^0, \qquad \tilde{M}^{0'} = -\tilde{T}^0, \qquad \tilde{U}^{0'} + \tilde{\theta}^0 = 0 \qquad (4\text{-}22)$$

The beam model (4-21), (4-22) combines features of the inner bending shear beam and of the slender-Timoshenko beam (for which $K_f/K_w = O(1)$ so that the shear force and the inner kinematic differ from the present case). We conclude that the double bending shear beam requires six macroscopic boundary conditions to be expressed with the above defined macroscopic variables.

Continuous family of macro behaviors. A systematic study demonstrates that the behaviors evolve gradually according to the properties of the frame elements. To illustrate this, let us fix the thickness of walls at $a_w/\ell_w = O(\varepsilon)$ and decrease the thickness of the floors. The following descriptions are obtained (for briefness, only the equations expressed with $\tilde{U}^0$ are given):

$$\frac{a_f}{\ell_w} = O(\varepsilon^{1/2}) : \quad E_w I\left(\tilde{U}^{0''''} + \frac{\Lambda_f \tilde{\omega}_{5/4}^2}{K_w} \tilde{U}^{0''}\right) = \Lambda_f \tilde{\omega}_{5/4}^2 \tilde{U}^0$$

$$\frac{a_f}{\ell_w} = O(\varepsilon) \quad : \quad E_w I\left(\tilde{U}^{0''''} + \frac{\Lambda \tilde{\omega}_1^2}{K} \tilde{U}^{0''}\right) = \Lambda \tilde{\omega}_1^2 \tilde{U}^0$$

$$\frac{a_f}{\ell_w} = O(\varepsilon^{3/2}) : \quad K_f \tilde{U}^{0''} + \Lambda_w \tilde{\omega}_{7/4}^2 \tilde{U}^0 = 0$$

$$\frac{a_f}{\ell_w} = O(\varepsilon^{5/3}) : \quad K_f \tilde{U}^{0''} + \Lambda_w \tilde{\omega}_2^2 \tilde{U}^0 = 2 E_w I_w \tilde{U}^{0''''}$$

$$\frac{a_f}{\ell_w} = O(\varepsilon^2) \quad : \quad \Lambda_w \tilde{\omega}_2^2 \tilde{U}^0 = 2 E_w I_w \tilde{U}^{0''''}$$

For floors thickness such that $a_f/\ell_w = O(\varepsilon^{1/2})$ or $O(\varepsilon)$, the global bending and shear of the cell (governed by the wall or the frame flexibility) are of the same magnitude and lead to slender Timoshenko models. The decrease of the floor thickness increases their flexibility and in turn prevents the global bending. Thus, in a first step, where $a_f/\ell_w = O(\varepsilon^{3/2})$, a shear beam governed by the floor flexibility is recorded; in a second step, where $a_f/\ell_w = O(\varepsilon^{5/3})$, the inner bending of walls appears leading to an inner bending / shear beam; and lastly, with $a_f/\ell_w = O(\varepsilon^2)$, the floor's participation (which only synchronize the wall motions) vanishes and an inner bending beam is obtained.

The second example concerns beams of identical walls and floors thickness. A continuous passage from the global bending beam (as a perforated beam) through a Timoshenko beam and finally a shear beam is observed when reducing the thicknesses:

$$\begin{cases} \dfrac{a_w}{\ell_w} = O\left(\dfrac{a_f}{\ell_f}\right) = O(\varepsilon^{1/2}) : & E_w I \tilde{U}^{0''''} = \Lambda \tilde{\omega}_1^2 \tilde{U}^0, \\[2mm] \dfrac{a_w}{\ell_w} = O\left(\dfrac{a_f}{\ell_f}\right) = O(\varepsilon) \quad : & E_w I\left(\tilde{U}^{0''''} + \dfrac{\Lambda \tilde{\omega}_1^2}{K} \tilde{U}^{0''}\right) = \Lambda \tilde{\omega}_1^2 \tilde{U}^0, \\[2mm] \dfrac{a_w}{\ell_w} = O\left(\dfrac{a_f}{\ell_f}\right) = O(\varepsilon^{3/2}) : & K \tilde{U}^{0''} + \Lambda \tilde{\omega}_{3/2}^2 \tilde{U}^0 = 0. \end{cases} \qquad (4\text{-}23)$$

To summarize, three elastic parameters determine the different macroscopic behaviors:

– the cell shear stiffness K, which may be reduced to the wall or floor stiffness (K_w or K_f);

- the global bending stiffness $E_w I$;

- the inner bending stiffness $2E_w I_w$.

Owing to scale separation, these parameters are given by the static properties of the elements (see (b) and (c) on page 1715). The scaling of the thicknesses (then stiffnesses) is essential to capture the physics and to identify all possible models. Without scaling, meaning in fact $a_w/\ell_w = O(a_f/\ell_f) = O(1)$, the only model that could be obtained would be a global bending model, irrelevant for most cases.

Despite a common architecture, the various structures exhibit very different dynamic behaviors: for instance, the eigenfrequencies f_k follow the series of odd integers, $f_k/f_1 = (2k-1)$ for cantilever shear beam and are approximately proportional to the series of square odd integers, $f_k/f_1 \approx (2k-1)^2/1.44$ $(k > 1)$, for the bending beam.

Generic beam model. The aim is to build a model that may degenerate to any of the previous model. To include all the mechanisms, such a model must involve the three kinematic variables U, α, θ. This generalization sacrifices the uniformity in order of magnitude of the several terms (i.e., according to the value of the parameters, some terms could be negligible in this generalized model). For this reason, the tilde and exponent order are removed from the variables. The natural way to associate in a generic beam the slender-Timoshenko and inner bending shear beam properties is to define the following behavior laws:

$$\begin{cases} \text{shear force} & T = -K(U' + \alpha) \\ \text{bending moment} & M = E_w I \alpha' \\ \text{inner moment} & \mathcal{M} = 2E_w I_w U'' \end{cases} \tag{4-24}$$

and the force and moment balance equations, associated with the inner kinematic of the section:

$$(T + \mathcal{M}')' = \Lambda \omega^2 U, \qquad M' = -T, \qquad K_w(U' + \theta) + K_f(\theta - \alpha) = 0. \tag{4-25}$$

Thus, the sixth order equation governing the generic beam takes the generalized form

$$\frac{2E_w I_w E_w I}{K} U'''''' - (2E_w I_w + E_w I) U'''' - \frac{E_w I}{K} \Lambda \omega^2 U'' + \Lambda \omega^2 U = 0. \tag{4-26}$$

Energy balance and boundary conditions. The consistency of those definitions can be checked by establishing the energy balance of this generic beam. For this purpose, multiply (4-25)a by U and integrate by part over the beam length H:

$$\int_0^H \Lambda \omega^2 U^2 dx = \int_0^H (T' + \mathcal{M}'') U dx = \left[(T + \mathcal{M}') U \right]_0^H - \int_0^H (T + \mathcal{M}') U' dx.$$

Taking into account (4-25)$_2$ and then integrating again by parts, the last integral becomes

$$\int_0^H T(U' + \alpha) dx + \int_0^H M' \alpha dx + \int_0^H \mathcal{M}' U' dx$$

$$= \int_0^H \left(T(U' + \alpha) - M\alpha' - \mathcal{M} U'' \right) dx + [M\alpha]_0^H + [\mathcal{M} U']_0^H.$$

Finally, using the behavior laws (4-24), we get

$$\int_0^H \Lambda\omega^2 U^2 \, dx = \underbrace{\int_0^H \left(\frac{T^2}{K} + \frac{M^2}{E_w I} + \frac{\mathcal{M}^2}{2E_w I_w}\right) dx}_{\text{Elastic energy}} + \underbrace{\left[(T + \mathcal{M}')U\right]_0^H - \left[M\alpha\right]_0^H - \left[\mathcal{M}U'\right]_0^H}_{\text{Work of boundary conditions}} \quad (4\text{-}27)$$

This energy balance equation states the equality of the kinetic energy with the elastic energy associated to the three mechanisms and the energy provided at the boundaries (which defines explicitly the appropriate boundary conditions). This suggests that, to define the macroscopic constitutive laws of the equivalent continuous beam, it is more general to use the three global cell parameters involved in the shear, global and inner bending rather than the precise frame cell geometry. When expressed with these global cell parameters, the beam-like descriptions established above may be employed for other symmetric cells, as explained in the next section.

5. Behavior of real structures

This section deals with practical applications of the preceding results. Real structures, made up of a finite (even if large) number of cells, themselves of finite size, match only imperfectly the homogenization conditions stipulating that the scale ratio should tend to zero.

As a first consequence, the homogenized descriptions only provide reasonable approximations to the behavior. What is meant by reasonable will be clarified in Section 5B, devoted to numerical modeling, and in Section 5C, where the effective order of the corrector is analyzed. A second consequence is of first importance for problems involving, in addition to the scale ratio, other small physical parameters (here the thickness to length ratios). For a given structure, what is the proper choice amongst the possible behaviors, or, in other words, what is the appropriate scaling?

5A. *Identification of the relevant modeling.* To establish the modeling, hence the proper scaling for a real structure, let's proceed as follows. Consider a given periodic structure of cell size ℓ, vibrating at macro scale and admit for the moment that the physical macro length L associated to these oscillations can be correctly assessed. Since ℓ is known, the *finite physical scale ratio*

$$\tilde{\varepsilon} = \frac{\ell}{L}$$

of this structure under these vibrations is therefore defined. The numerical finite value of each small parameter (here geometrical) characterizing the real cell can also be quantified and equalized to the physical scale ratio $\tilde{\varepsilon}$ at a particular power. This power, then replaced by a close integer or rational number, supply unambiguously the physical scaling consistent with the real problem in consideration.

Performing homogenization with this scaling consists in replacing the physical value $\tilde{\varepsilon}$ by a mathematical ε tending to zero. By doing so, the relative orders of magnitude of the physical terms are kept identical from the real cell to the continuous model obtained at the limit. Finally, the real structure can be seen as an imperfect realization (for the small but finite mathematical value $\varepsilon = \tilde{\varepsilon}$) of the homogenized continuous model built with the proper scaling. The smaller $\tilde{\varepsilon}$ is, the better would be the continuous approximation. Thus, in real cases it is possible to identify the right continuous description, provided that the macro length L is reliably estimated.

Macroscopic length of modal vibrations. Length L is evaluated by a dimensional analysis realized at the macroscopic scale, which gives classically [Boutin and Auriault 1990]

$$L = \frac{O(U)}{O(\partial_x U)} \tag{5-1}$$

This estimation is consistent with the asymptotic expansion since the increment of the macroscopic variable on one cell, $\ell\,\partial_x U$, has to be of order ε compared to its current value, U. This implies: $\ell\,\partial_x U = O(\varepsilon\,U) = O(\ell\,U/L)$, leading to (5-1). Apply this result to the k-th eigenmode of cantilever beams (embedded at base and free at the top) of length H (the cantilever conditions are taken for concreteness):

– For shear beams, the modal analysis shows that modal shape are expressed on the basis of two exponentials $\{e^{(\pm ix/L_k)}\}$, L_k being solutions of $\cos(H/L_k) = 0$ so that $L_k = 2H/(\pi(2k-1))$. From the estimation (5-1), L_k is the researched characteristic length of the k-th mode of shear beams.

– For bending beams, the decomposition basis is $\{e^{(\pm ix/L_k)}, e^{(\pm x/L_k)}\}$, where L_k is a solution of $\cos(H/L_k) = 1/\cosh(H/L_k)$, whose zeros are close to $L_k \simeq 2H/(\pi(2k-1))$. Here again from (5-1), L_k is the characteristic length of the k-th mode of bending beams.

– For other beams combining shear and one (or two) bending effects, two (or three) spatial constants appear in the basis of exponentials. It can be proved algebraically that the smaller value (which must be considered for defining the characteristic length) is always close to $L_k \simeq 2H/(\pi(2k-1))$.

Thus, for an N-level structure ($H = N\,\ell_w$) and *independently of the model*, the macroscopic length L_k of the k-th embedded-free mode is known and the physical scale parameter is related to the mode number and to the number of cells:

$$\tilde{\varepsilon}_k = \frac{\ell}{L_k} \simeq \frac{\pi(2k-1)}{2N}, \qquad L_k \simeq \frac{2H}{\pi(2k-1)} \tag{5-2}$$

To illustrate (5-2), consider the first mode of a ten-level building as in Figure 1. From (5-2) $\tilde{\varepsilon}_1 = 0.15$ and if $\ell_w = \ell_f = 3\,\text{m}$ and $a_w = a_f = 50\,\text{cm} = O(\tilde{\varepsilon}_1\ell_w)$, a slender-Timoshenko beam is expected. If $a_w = a_f = 20\,\text{cm} = O(\tilde{\varepsilon}_1^{1.5}\ell_w)$, the behavior would be that of a shear beam, and so on.

Interestingly, (5-2) indicates that the maximum number of modes respecting the scale separation is limited to $N/3$ (a third of the number of cells), beyond which HPDM is irrelevant.

Identification criterion based on dimensionless parameters. To identify the global behavior of a given structure, more physical insight, as well as generality, would be obtained by working in terms of macroscopic elastic coefficients of the cell rather than in terms of its elements thicknesses. In this aim, since the macro lengths are quite similar whatever the modeling, a dimensional analysis is realized on the generic beam. The change of variables $\boldsymbol{x} = x/L$ (with the mode to be specified later) transforms the governing equation (4-26) into

$$C\,\gamma\,U^{*''''''} - (1+\gamma)\,U^{*''''} - \Omega^2\,U^{*''} + \frac{\Omega^2}{C}\,U^* = 0, \tag{5-3}$$

where, by construction, the dimensionless terms marked with $*$ are $O(1)$ and

$$C = \frac{E_w I}{K L^2}, \qquad \gamma = \frac{2 E_w I_w}{E_w I} = \frac{2 I_w}{I}, \qquad \Omega^2 = \frac{\Lambda \omega^2 L^2}{K}. \tag{5-4}$$

C evaluates the global bending effect compared to shear effect and γ the inner bending compared to global bending. C and γ supply efficient identification criteria of behavior: according to their order of magnitude with respect to $\tilde{\varepsilon}$, Equation (5-3) degenerates into simplified forms in such a way that all the models are recovered. For instance, if $C = O(1)$ and $\gamma = O(\tilde{\varepsilon})$, the terms related to $C\gamma$ and γ disappear and the resulting model is

$$U^{*''''} + \Omega^2\, U^{*''} - \frac{\Omega^2}{C}\, U^* = 0,$$

which corresponds to a slender Timoshenko beam, and similarly for the other cases. By doing so, seven behaviors are obtained depending on the value of C, $C\gamma$ and γ compared to $\tilde{\varepsilon}$ and $\tilde{\varepsilon}^{-1}$. A synthetic representation (Figure 3) is deduced by mapping the domain of validity of each behavior according to the two parameters p and q defined by

$$C = \tilde{\varepsilon}^p \quad \text{and} \quad \gamma = \tilde{\varepsilon}^q. \tag{5-5}$$

We remark that γ and the constant β defined by

$$\beta = \frac{E_w I}{K\ell_w^2} = \frac{E_w I}{KL^2}\left(\frac{L}{\ell_w}\right)^2 = C\,\tilde{\varepsilon}^{-2} = \tilde{\varepsilon}^{\,p-2} \tag{5-6}$$
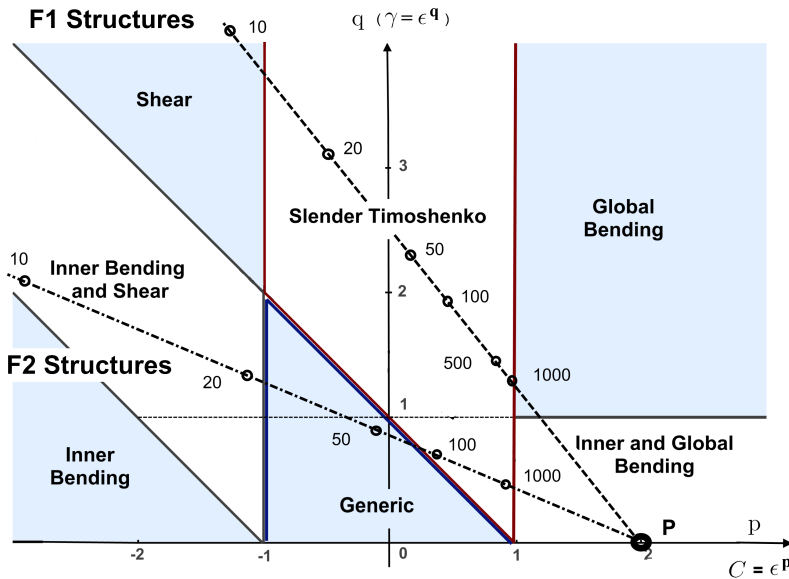
Figure 3. Domains of validity of the equivalent beams according to values of p and q defined by $C = \tilde{\varepsilon}^p$ and $\gamma = \tilde{\varepsilon}^q$. Beams made of a given cell are located on a straight line issued from point P ($p = 2$, $q = 0$). On this line, the representative point moves away from P when increasing the order k of the mode and closer to P when increasing the number N of cells. For example, the two dotted straight lines correspond to the behavior of the first mode in function of the number of levels (numbered points) for the F_1 and F_2 structures studied in Section 5B.

provide two intrinsic parameters of the cell (for the structures being studied, $a_w < \ell_w = O(\ell_f)$ implies $\gamma < 1$). Therefore, values of p and q enabling one to define the behavior of beams made of a *given cell* (β and γ fixed) are determined in the following manner: in terms of $\tilde{\varepsilon}$ — which depends on the number of cells and on the mode number; see (5-2) — p and q are given by

$$(p-2)\log\tilde{\varepsilon} = \log\beta \quad \text{and} \quad q\log\tilde{\varepsilon} = \log\gamma;$$

then, eliminating $\tilde{\varepsilon}$, we get

$$(p-2)\log\gamma - q\log\beta = 0. \tag{5-7}$$

Thus, in the (p,q) plane, the possible behaviors of beams made of a *given cell* necessarily lie on the straight line issuing from point P $(p=2, q=0)$ of (5-7). For beams made of a given number of cells, the position on the line moves away from P as the mode number is increased ($\tilde{\varepsilon}$ increases). Conversely, for a given mode number, the position on the line approaches P as the number of cells increases (and $\tilde{\varepsilon}$ decreases). Consequently, the modes of a given structure are not necessarily described by a unique macroscopic model. For instance, the description could be a bending beam for the first few modes, then a slender-Timoshenko beam and finally a shear beam for the higher modes: see Figure 3. Conversely, at a given mode order, if the number of cells is increased, the opposite evolution from shear to bending beam arises. This corresponds to the well known effect of slenderness in beam theory.

5B. *Numerical validation.* To investigate the relevance of the homogenized descriptions for structures of finite number of cells, we made comparisons with numerical simulations. We modeled a large number of fictitious structures, each made of basic frames having walls and floor of length 3 m and modulus $E = 200\,\text{GPa}$. The diversity that allows most of the cases to be covered was introduced in two ways. First, the number N of cells varies from 5 to 1000; secondly, two basic frame have been used:

– F_1, whose walls and floor thicknesses are identical (0.1 m), and

– F_2, whose walls are thicker (1 m) than the floor (0.15 m).

For each of these structures, considering clamped-free boundary conditions, the four first eigenmodes were calculated using three independent methods:

– First, a direct numerical treatment of the structure was carried out with the finite element code RDM6, using a beam element for meshing each beam of the structure. The convergence criterion was based on the relative eigenfrequency error being less than 10^{-4}.

– Next, the eigenmodes were determined using generic beam modeling, with appropriate intrinsic parameters for the basic frames ($\beta = 675$ and $\gamma = 1/2700$ for F_1, and $\beta = 1336$ and $\gamma = 1/27$ for F_2) and appropriate boundary conditions ($U = 0$, $\alpha = 0$, $\theta = 0$ on the clamped base, and $T = 0$, $M = 0$, $\mathcal{M} = 0$ on the top). The resolution (not presented here) followed the modal method; the eigenfrequencies are the zeros of the 6×6 determinant of equations describing the boundary conditions.

– Finally, the proper modeling of each structure is identified from the calculated values of C and γ, compared to $\tilde{\varepsilon} = \pi/2N$ power. The proper boundary conditions are expressed with the macro variables of the identified model, and the eigenmodes are determined; following this approach, F_1-structures are always well modeled by a slender-Timoshenko beam, but simpler models are efficient: shear beam when $N < 30$; global bending beam when $N > 300$ (Figure 6, top). The F_2-structures vary from an
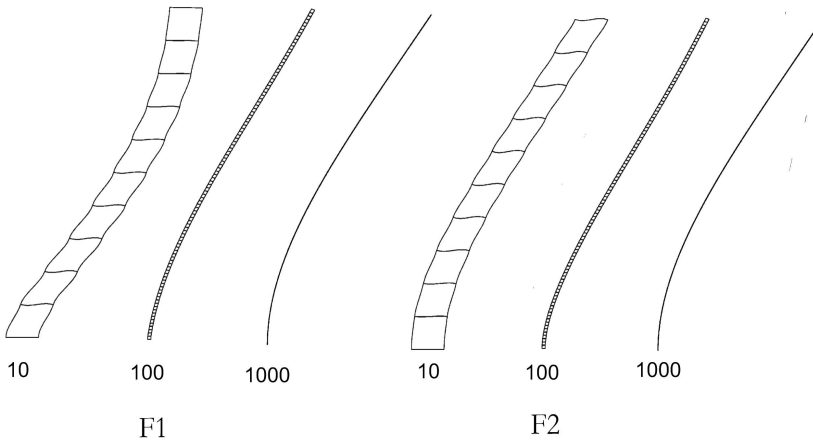
Figure 4. Fundamental mode shape of F_1-structures (left) and F_2-structures (right) made of 10, 100 or 1000 identical frames. For comparison, all the structures are drawn at the same size.

inner bending beam ($N < 20$) to a generic beam close to a shear beam ($N \approx 60$) and tend to a global bending beam for $N > 200$ (Figure 3 and 6, bottom).

The analysis of the results focuses on three points:

(1) the diversity of behaviors, illustrated by the variety of the mode shapes (Figure 4),

(2) a comparison of the eigenfrequencies derived by the three methods (Figures 5 and 6), and

(3) the series of eigenfrequency ratios f_i/f_1 for $i = 2, 3, 4$ (Figure 6). This series of ratios characterizes very efficiently the nature of the behavior, and so constitutes a stringent criterion for the reliability of equivalent beams. Shear and bending beams correspond respectively to the series $(1, 3, 5, 7)$ and $(1, 6.25, 17.36, 34.03)$.

Figure 5 shows excellent agreement of the generic beam modeling with the numerical calculations. This highlights the relevance of the analytical generic beam for the wide range of cases we tested. Even with poor scale separation (and even very poor, e.g., the fourth mode of the five-frame structure), the generic beam provides surprisingly good results. An attempt to explain this observation is made in Section 5C.

The comparison in Figure 6 between the results derived from the proper specific beam and the generic beam (and numerical modeling) shows that both coincide only in the validity range established theoretically. As expected, outside this range, both significantly diverge, meaning that the specific model loses its relevancy, and has to be replaced by the actual proper beam in this other range. The continuous evolution from one model to another is consistent with that predicted above (Figure 3). To summarize:

– In the scale separation frequency range, the tested structures reach most of the possible cases (shear, slender-Timoshenko, double bending, generic beam); it appears that every case can be described accurately by one of these modeling, meaning that all the physical mechanisms are properly described by the homogenized behavior.
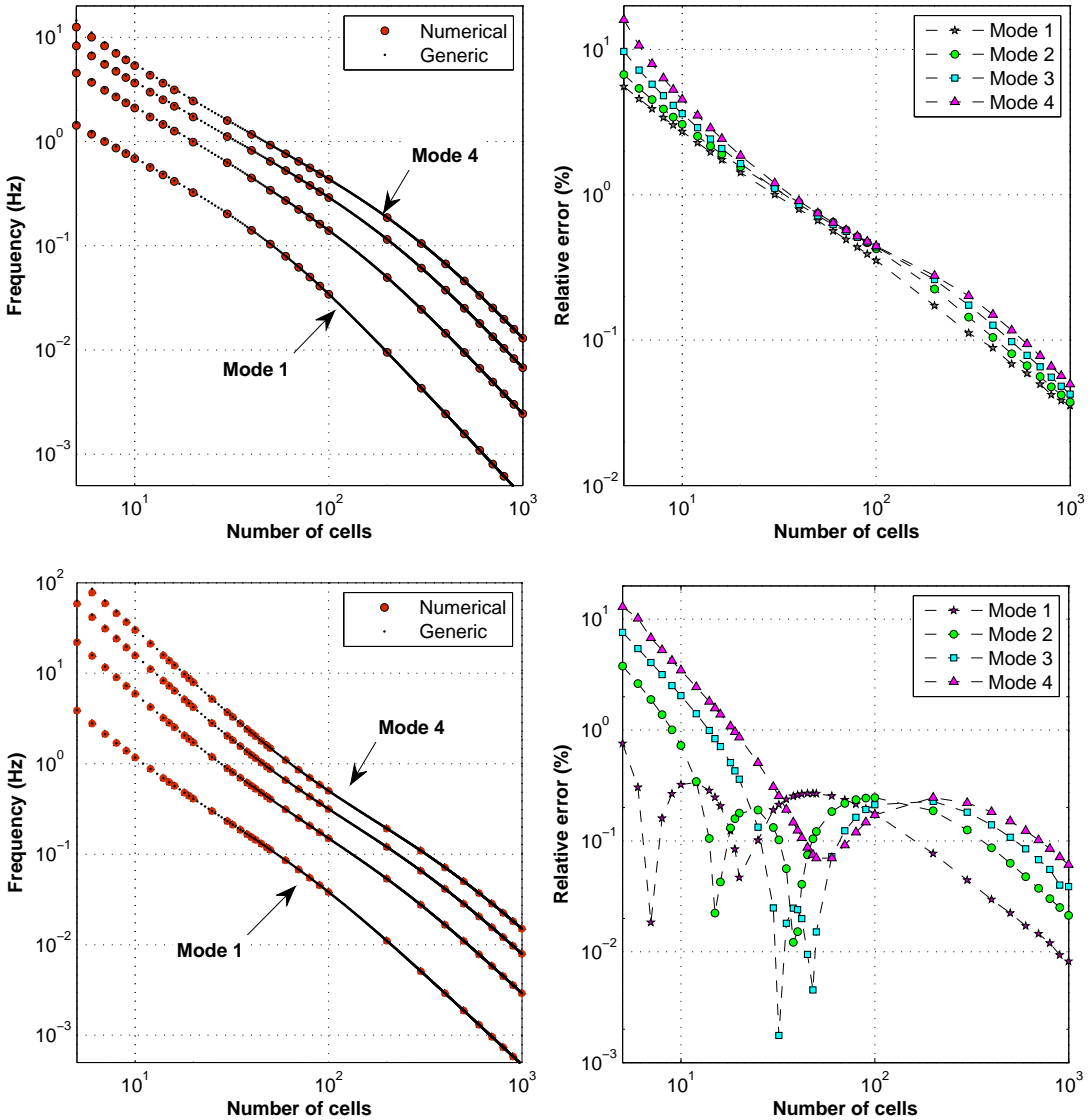
Figure 5. Eigenfrequencies of the four first modes of F_1 structures (top) and F_2 structures (bottom), versus the number of frames. Comparison between generic beam modeling and numerical calculations (left) and errors evaluation in percent (right).

– The interest and the accuracy of the generic beam clearly appears, specially in intermediate cases where none of the simplified beams provides sufficiently accurate results.

– The proposed procedure of determining the proper macro beam for a specific case is confirmed numerically.

– Complementary to the generic beam, the interest and the accuracy of the relevant homogenized beam model, of easier use than the generic beam model, are confirmed in their own validity range.
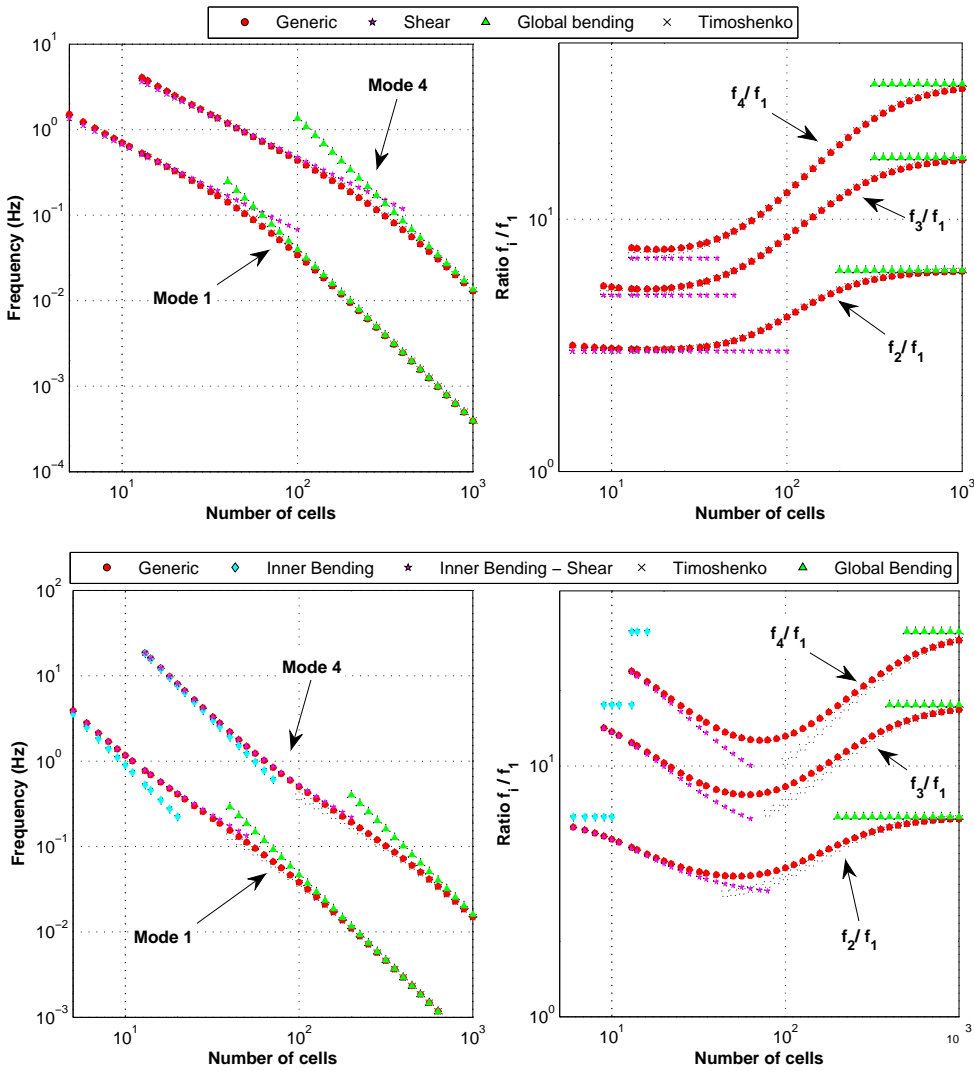
Figure 6. Comparison between generic beam modeling and identified proper beam model (top: shear and slender-Timoshenko, F_1-structures; bottom: inner bending beam and global bending, F_2-structures). On the left are shown the eigenfrequencies of the first and fourth modes; other modes are not drawn for the clarity. On the right, ratios f_i/f_1 versus the number of frames.

5C. *Effective corrector order: the slender-Timoshenko case.* The numerical examples have shown that HPDM provides accurate results even though the scale separation is poor. A possible explanation may be found in the effective order of magnitude of the terms neglected by the zero order description. In fact, despite the form of the expansion (2-1), it will be shown that the corrector is of order ε^2 (at least for slender-Timoshenko beams). This argument is in favor of a largest extent of validity and reliability of the homogenized description.

Investigate high order terms for improving the description in the presence of poor scale separation have already been proposed for continuous media [Bensoussan et al. 1978; Bakhvalov and Panasenko 1989; Gambin and Kröner 1989; Boutin and Auriault 1993], for discrete media [Verna 1991; Tollenaere 1994; Pradel and Sab 1998] and for beams [Buannic and Cartraud 2001a; 2001b]. A detailed analysis of higher order correctors is beyond the scope of this paper; the single case of the slender-Timoshenko beam is studied hereafter to identify its effective order.

Macroscopic balance equations at the first order. To pursue at the next order the resolution begun in Section 4 and Section 7, the balance equations concerning $\tilde{U}^1$, $\tilde{\theta}^1$, $\tilde{\alpha}^1$ are established, whose beam theory interpretation is similar to that of the zero order. The behavior laws remain identical:

$$\tilde{T}^1 = -K\left(\tilde{\alpha}^1 + \tilde{U}^{1'}\right), \qquad \tilde{M}^1 = E_w I\, \tilde{\alpha}^{1'}, \tag{5-8}$$

whereas the balance equations read ($\tilde{\omega}_2$ is the second term of the modal frequency expansion):

$$\tilde{T}^{1'} - \Lambda\tilde{\omega}_1^2\, \tilde{U}^1 = 2\Lambda\tilde{\omega}_1\tilde{\omega}_2\, \tilde{U}^0, \qquad \tilde{M}^{1'} = -\tilde{T}^1. \tag{5-9}$$

The difference with (4-11) comes from the term induced by the zero order solution $\tilde{U}^0$, playing the role of an inner body force. Combining (5-8) and (5-9), we see that the first order is governed by

$$\Gamma[\tilde{U}^1] = E_w I\left(\tilde{U}^{1''''} + \frac{\Lambda\tilde{\omega}_1^2}{K}\, \tilde{U}^{1''}\right) - \Lambda\tilde{\omega}_1^2\, \tilde{U}^1 = \frac{2\tilde{\omega}_2}{\tilde{\omega}_1} E_w I\, \tilde{U}^{0''''}, \tag{5-10}$$

where the differential operator Γ is the same as at the zero order; see (4-9).

Cancellation of the first order. The first corrective term generally presents a particular energetic property. In composite media, the work of the first corrector under the zero order solution is null at the period scale; see for example [Boutin and Auriault 1993; 1995]. For discrete media, a similar result was obtained for braced framed structures in [Tollenaere 1994].

This property is related to the Fredholm alternative [Bensoussan et al. 1978]. In fact, the order zero solution is the eigenfunction associated to the null eigenvalue of the differential operator. This latter being unmodified at the next order, a solution exists if and only if the source term is orthogonal to the eigenfunction with eigenvalue zero, which is the order zero solution.

We apply this idea here by calculating the virtual work of $\tilde{U}^0$ under $\tilde{U}^1$ and reciprocally, these motions being governed by

$$\Gamma[\tilde{U}^0] = 0, \qquad \Gamma[\tilde{U}^1] = \frac{2\tilde{\omega}_2}{\tilde{\omega}_1} E_w I\, \tilde{U}^{0''''}. \tag{5-11}$$

For simplicity we consider cantilever beams, so the energy at the boundary conditions cancels out. Algebra similar to that presented in Section 4 gives

$$\int_0^H \Gamma[\tilde{U}^0]\, \tilde{U}^1 dx = W(\tilde{U}^0, \tilde{U}^1) + E_c(\tilde{U}^0, \tilde{U}^1) = 0 \tag{5-12}$$

and

$$\int_0^H \left(\Gamma[\tilde{U}^1] - \frac{2\tilde{\omega}_2}{\tilde{\omega}_1} E_w I\, \tilde{U}^{0''''}\right)\tilde{U}^0 dx = W(\tilde{U}^0, \tilde{U}^1) + E_c(\tilde{U}^0, \tilde{U}^1) + \int_0^H 2\Lambda\tilde{\omega}_1\tilde{\omega}_2\, (\tilde{U}^0)^2 dx = 0, \tag{5-13}$$

where the elastic energy W and the virtual kinetic energy E_c take on the form

$$W\left(\tilde{U}^0, \tilde{U}^1\right) = \int_0^H \left(\frac{\tilde{T}^0 \tilde{T}^1}{K} + \frac{\tilde{M}^0 \tilde{M}^1}{E_w I}\right) dx, \qquad E_c\left(\tilde{U}^0, \tilde{U}^1\right) = \int_0^H \Lambda \tilde{\omega}_1^2 \, \tilde{U}^0 \, \tilde{U}^1 dx.$$

Comparison of (5-12) and (5-13) leads directly to $\tilde{\omega}_2 = 0$, and then the source term induced by $\tilde{U}^0$ cancels out in the first order balance (5-11)$_2$. Therefore the equations describing the zero and first order are identical, and the first order can be set to zero without restriction. Consequently, the first corrector of the continuous description is only $O(\varepsilon^2)$. It can be inferred from the general argument of the demonstration that this still holds in the other cases.

6. Analogy with micromorphic media

This section points out an analogy between the derived beam behavior and the behavior of micromorphic materials [Eringen 1968]. Toward this aim, we use the physical insight gathered from the dimensional analysis of one-dimensional periodic structures to investigate the features of bi-dimensional periodic structures. For convenience this section focuses on the first mode of transverse vibration polarized in the direction e_2, propagating in the direction e_1. Similar arguments apply for higher modes.

From one- to two-dimensional structures. Consider a cell F_{rame} of shear stiffness K, inner bending stiffness $E I_w$ and global bending stiffness $E I$ corresponding to the intrinsic coefficients $\beta = E I / K \ell_w^2$ and $\gamma = I_w / I$. From this frame, build a periodic $B_{eam} = N_{e_1} \times F_{rame}$, made of N_{e_1} frame cells repeated in the direction e_1, as in Figure 1. The first transverse mode behavior of the B_{eam} is driven by
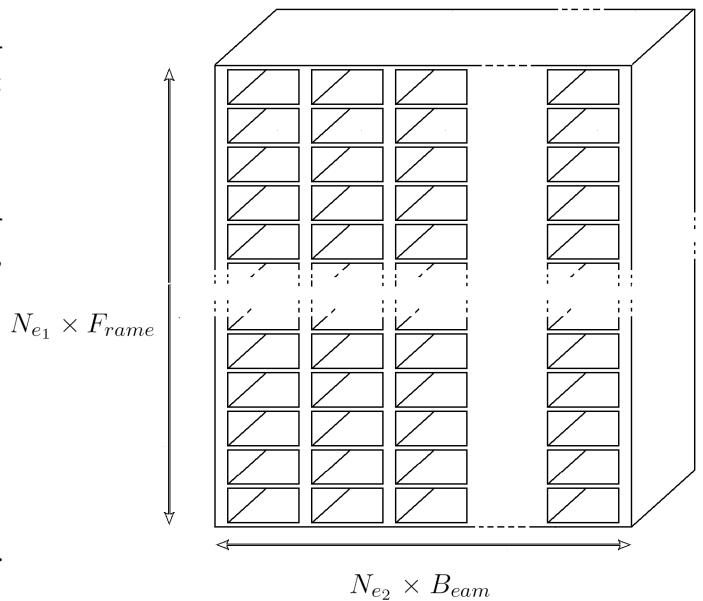
$$C_B = \beta \left(\frac{\pi}{2N_{e_1}}\right)^2, \qquad \gamma_B = \gamma.$$

Now build the two-dimensional periodic $S_{tructure}$ by repeating N_{e_2} times in the transverse direction e_2 the same primitive B_{eam}:
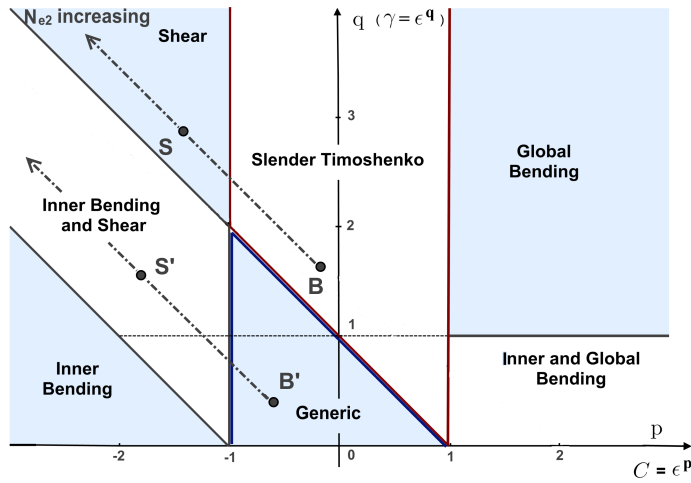
$$S_{tructure} = N_{e_2} \times B_{eam} = N_{e_1} \times (N_{e_2} \times F_{rame}).$$

(See figure on the right.) Taking advantage of the periodicity in the e_1 direction, apply to this $S_{tructure}$ the one-dimensional homogenization process.

The properties of the cell made of N_{e_2} copies of F_{rame} (with $N_{e_2} + 1$ walls) can be estimated from those of the basic frame F_{rame}: the shear stiffness is $O(N_{e_2} K)$, the inner bending stiffness is $O(N_{e_2} E I_w)$, and the global bending stiffness is $O(N_{e_2}^3 E I)$. Thus the behavior of $S_{tructure}$ under the first

$N_{e_1} \times F_{rame}$

$N_{e_2} \times B_{eam}$

Figure 7. Behavior of the $S_{tructure} = N_{e_2} \times B_{eam}$ in relation to that of the primitive $B_{eam} = N_{e_1} \times F_{rame}$.

transverse mode is driven by the two dimensionless parameters related to those of the primitive frame F_{rame}:

$$C_S = \left(\frac{\pi N_{e_2}}{2N_{e_1}}\right)^2 \beta > C_B, \qquad \gamma_S = \left(\frac{1}{N_{e_2}}\right)^2 \gamma < \gamma_B, \qquad C_S \gamma_S = C_B \gamma_B = \left(\frac{\pi}{2N_{e_1}}\right)^2 \beta \gamma. \tag{6-1}$$

The scale ratio is the same for both B_{eam} and $S_{tructure}$, since they have the same number N_{e_1} of cells in the direction e_1:

$$\tilde{\varepsilon}_S = \tilde{\varepsilon}_B = \tilde{\varepsilon} = \pi/(2N_{e_1}).$$

Therefore, introducing (p_S, q_S) and (p_B, q_B) such that

$$C_S = \tilde{\varepsilon}^{\ p_S}, \quad \gamma_S = \tilde{\varepsilon}^{\ q_S}, \quad C_B = \tilde{\varepsilon}^{p_B}, \quad \gamma_B = \tilde{\varepsilon}^{q_B},$$

the relations (6-1) lead to $p_S + q_S = p_B + q_B$, $p_S < p_B$, and $q_S > q_B$, meaning that in the plane (p, q) of Figure 7, the points S (p_S, q_S) and B (p_B, q_B) representing $S_{tructure}$ and B_{eam} lie on the diagonal of slope -1 going through B. According to the results of Section 5A, the behaviors of the B_{eam} and $S_{tructure}$ are of the same nature if $p_B \le -1$, but may differ if $p_B > -1$.

Micromorphic media. Consider a L_{ayer} of a "cellular material" of finite thickness $N_{e_1}\ell_w$ and infinite length by making N_{e_2} tend to ∞. From the same reasoning, the point L (p_L, q_L) representative for the L_{ayer} submitted to transverse motion of infinite lateral extent is such that

$$p_L + q_L = p_B + q_B, \qquad |p_L|, q_L \to +\infty.$$

Two possibilities appear (see Figure 7):

− $C_B \gamma_B \le \tilde{\varepsilon} = \pi/(2N_{e_1})$. The behavior of the L_{ayer} is necessarily that of a shear beam. The single remaining macroscopic kinematic variable is the translation, which satisfies periodicity in the two directions. Thus, at the leading order the layer behaves as a classical Cauchy medium, as could be derived via two-dimensional periodic homogenization. (For the cell under study, this case occurs when
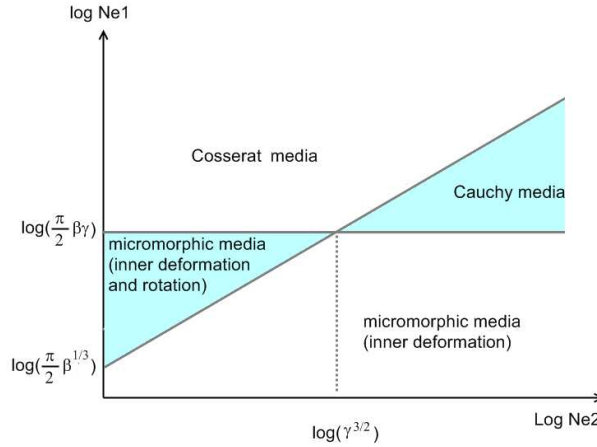
Figure 8. Macroscopic behaviors of a medium whose basic frame is characterized by the intrinsic parameters β and γ, when submitted to a shear in the direction e_1 polarized in the direction e_2 acting on the $D_{omain} = N_{e_2} \times N_{e_1} \times F_{rame}$.

the properties of the elements of the frame are of the same order: an isotropic or weakly anisotropic cellular material.)

– $C_B \gamma_B \geq \tilde{\varepsilon} = \pi/(2N_{e_1})$. In this case, the L_{ayer} tends to behave as an inner bending beam (with or without shear). The description requires that the translation and the inner deformation both satisfy periodicity in the two directions. The inner deformation introduces local rotation (θ) *inside* the cell, but no rigid body rotation of the cell itself ($\alpha = 0$). Thus, this micromorphic behavior is neither that of a Cauchy medium nor that of a Cosserat material. (For the cell under study, this case requires walls significantly stiffer than the floor: a strongly anisotropic cellular material.)

Finally, consider an infinite media made of the frame F_{rame} and assume that, in a D_{omain} restricted to $N_{e_2} \times N_{e_1} \times F_{rame}$, appropriate boundary conditions impose normally to the direction e_1 a shear polarized in the direction e_2. The equivalent behavior of the medium in the D_{omain} is given by comparing the two parameters

$$C_D = \left(\frac{\pi N_{e_2}}{2N_{e_1}}\right)^2 \beta, \qquad \gamma_D = \left(\frac{1}{N_{e_2}}\right)^2 \gamma$$

with the power of $\tilde{\varepsilon}$. Four behaviors (see Figure 8) can occur, according to the independent kinematic variable(s):

(1) The sole kinematic variable is the translation U. This situation (shear beams) is observed when $C_D \gamma_D \leq \tilde{\varepsilon}$ and $C_D \geq \tilde{\varepsilon}^{-1}$. In terms of domain geometry, these conditions require, in the direction normal to the shear motion, that

$$N_{e_1} \geq \beta \gamma \pi/2$$

(i.e., a number of cells higher than the intrinsic critical number $\frac{1}{2}\pi\beta\gamma = EI_w/K\ell_w^2$) and, in the direction of the shear motion, that

$$N_{e_2} \geq \left(\frac{\pi}{2}N_{e_1}\right)^{3/2} \frac{1}{\sqrt{\beta}},$$

(i.e., a weak slenderness whose aspect ratio is governed by N_{e_1} and $\beta = EI/K\ell_w^2$). The equivalent continuum behavior within the domain is that of a Cauchy medium.

(2) The kinematic variables are the translation U and the inner rotation θ. This occurs when $C_D\gamma_D \geq \tilde{\varepsilon}$ and $C_D \geq \tilde{\varepsilon}^{-1}$ (inner bending beam with or without shear), which means

$$N_{e_1} \leq \frac{\pi}{2}\beta\gamma, \qquad N_{e_2} \geq \left(\frac{2}{\pi}N_{e_1}\right)^{3/2}\frac{1}{\sqrt{\beta}}.$$

The equivalent continuum behavior within the domain is that of a micromorphic medium with inner deformation.

(3) The kinematic variables are the translation U and the rotation α. This happens when $C_D\gamma_D \leq \tilde{\varepsilon}$ and $C_D \leq \tilde{\varepsilon}^{-1}$ (slender-Timoshenko and bending beams), i.e.,

$$N_{e_1} \geq \frac{\pi}{2}\beta\gamma, \qquad N_{e_2} \leq \left(\frac{2}{\pi}N_{e_1}\right)^{3/2}\frac{1}{\sqrt{\beta}}.$$

In this case the cell rotation breaks the lateral periodicity, whereas the periodicity in the perpendicular direction is kept. For this reason, such a phenomenon is not be described by the usual two-dimensional homogenization (which would impose the periodicity in both directions). Nevertheless, the deformation presents a scale separation in a single direction that enables the treatment by a one-dimensional homogenization. In such a domain, the effects of global bending and shear are of same order and the medium behaves as a Cosserat medium.

(4) Finally, all three variables U, α and θ can be kinematic variables; this situation obtains when $C_D\gamma_D \geq \tilde{\varepsilon}$ and $C_D \leq \tilde{\varepsilon}^{-1}$ (generic beam). This is possible only for a restricted domain geometry defined by

$$N_{e_1} \leq \frac{\pi}{2}\beta\gamma, \qquad N_{e_2} \leq \left(\frac{2}{\pi}N_{e_1}\right)^{3/2}\frac{1}{\sqrt{\beta}}.$$

The behavior is that of a complex micromorphic medium with inner deformation and rotation. Such behavior cannot be derived if the periodicity is assumed in both directions.

Note that to respect the scale separation, the micromorphic behavior with inner deformation can only be observed if the critical number $\frac{1}{2}\pi\beta\gamma$ is significantly larger than 1 (referring to the frames studied in Section 5B, this is the case for F_2 but not for F_1). Cells such that $\frac{1}{2}\pi\beta\gamma \gg 1$ require a lack of diagonal bracing, since a diagonal element, which works in extension and prevents the cell flexibility, increases considerably the shear stiffness up to $K = O(E\ell^2)$ and the global and inner bending become of the same order, so that $\beta = O(1)$, $\gamma = O(1)$ and $\frac{1}{2}\pi\beta\gamma = O(1)$.

7. Implementing HMPD for framed structures

This section revisits in some detail the homogenization of the class of structures considered. Sections 7A–7D are an exposition of the discrete formulation of the global dynamic balance equations, following [Tollenaere 1994]. This material is then developed for square lattice beams in 7E and applied to the case of a slender-Timoshenko beam in 7F.
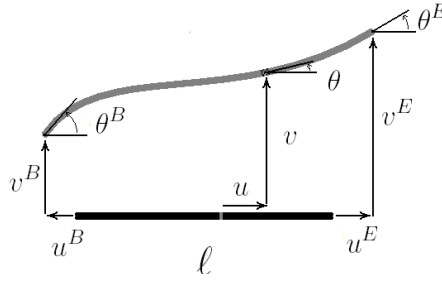
Figure 9. Notation for the deformation of a beam element in the plane (e_1, e_2).

7A. *Local balance of the elements.* Consider a beam element from point B to point E, of length ℓ, section A, and inertia I_b (Figure 9). In the local beam frame, s stands for the coordinate along the axis, and u, v, θ for the axial and transverse displacements and the rotation respectively. No external force is applied along the beam and the axial force N, the shear force T and the bending moment M act by convention from the left part to the right part. To describe global vibrations at the (unknown) modal frequencies $f = \omega/2\pi$ of the whole structure, any variable reads $Q(s, t) = Q(s)\, e^{i\omega t}$. By linearity, the time dependence is systematically simplified.

For longitudinal vibrations, the balance on the beam axis e_1, together with the compression behavior, can be written as

$$\text{N}'(s) = \rho A \omega^2 u(s), \qquad \text{N}(s) = -E A u'(s) \tag{7-1}$$

(primes stands for differentiation with respect to s). This leads to the governing equation

$$\ell_L^2 u''(s) = -u(s), \quad \text{where } \ell_L = \sqrt{E/\rho \omega^2}. \tag{7-2}$$

The compression wavelength of the element is $2\pi \ell_L$.

For transverse (bending) vibrations, we have the balance of shear force of axis e_2 and moment of axis e_3, plus the bending behavior law:

$$\text{T}'(s) = \rho A \omega^2 v(s), \qquad \text{M}'(s) = -\text{T}(s), \qquad \text{M}(s) = -E I_b v''(s). \tag{7-3}$$

Together these yield

$$\ell_T^4 v''''(s) = v(s), \quad \text{where } \ell_T = \sqrt[4]{E I_b / \rho A \omega^2}. \tag{7-4}$$

The transverse bending wavelength of the element is $2\pi \ell_T$. The longitudinal and transverse wavelengths are linked by the purely geometric relationship

$$\frac{\ell_T^4}{\ell_L^2} = \frac{I_b}{A}. \tag{7-5}$$

7B. *Nodal forces and moment.* Now integrate equations (7-2) and (7-4) between the origin B and the end E using the unknown displacements u^B, u^E, v^B, v^E and rotations θ^B and θ^E of the endpoints as boundary conditions (Figure 9). The forces at the endpoints, expressed in the local frame of the element

and deduced from the beam behavior laws, take on the form

$$
\begin{aligned}
N^B &= N(u^B, u^E), & N^E &= -N(u^E, u^B), \\
T^B &= T(v^B, v^E, \theta^B, \theta^E), & T^E &= -T(v^E, v^B, -\theta^E, -\theta^B), & \text{(7-6)} \\
M^B &= M(v^B, v^E, \theta^B, \theta^E), & M^E &= M(v^E, v^B, -\theta^E, -\theta^B),
\end{aligned}
$$

where we have set, with $\ell_i^* = \ell/\ell_i$, $c_i^* = \cos \ell_i^*$, $s_i^* = \sin \ell_i^*$, $ch_i^* = \cosh \ell_i^*$, $sh_i^* = \sinh \ell_i^*$ $(i = T, L)$,

$$
N(u_1, u_2) = \frac{EA}{\ell_L} \frac{u_1 \cos(\ell_L^*) - u_2}{\sin \ell_L^*},
$$

$$
T(v_1, v_2, \theta_1, \theta_2) = \frac{EI_b}{\ell_T^3} \frac{v_1(ch_T^* s_T^* + sh_T^* c_T^*) - v_2(s_T^* + sh_T^*) + \big(\theta_1 s_T^* sh_T^* - \theta_2(c_T^* - ch_T^*)\big)\ell_T}{c_T^* ch_T^* - 1}, \quad \text{(7-7)}
$$

$$
M(v_1, v_2, \theta_1, \theta_2) = \frac{EI_b}{\ell_T^2} \frac{v_1 s_T^* sh_T^* + v_2(c_T^* - ch_T^*) + \big(\theta_1(ch_T^* s_T^* - sh_T^* c_T^*) - \theta_2(s_T^* - sh_T^*)\big)\ell_T}{1 - c_T^* ch_T^*}.
$$

7C. *Discrete dynamic balance.* To express the node balance of the whole structure, the geometry of the frame is explicitly used. Level n contains two nodes (Figure 1): node n_1 on the left (end of wall wn_1, origin of wall $w(n+1)_1$ and of floor fn) and node n_2 on the right (end of wall wn_2 and floor n, origin of wall $w(n+1)_2$). The equilibrium of the forces (in directions e_1 and e_2) and the moment (e_3) read at any level n:

Node n_1: $T^E_{wn_1} - T^B_{w(n+1)_1} - N^B_{fn} = 0$, $N^E_{wn_1} - N^B_{w(n+1)_1} - T^B_{fn} = 0$, $M^E_{wn_1} - M^B_{w(n+1)_1} - M^B_{fn} = 0$,   (7-8)

Node n_2: $T^E_{wn_2} - T^B_{w(n+1)_2} + N^E_{fn} = 0$, $N^E_{wn_2} - N^B_{w(n+1)_2} + T^E_{fn} = 0$, $M^E_{wn_2} - M^B_{w(n+1)_2} + M^E_{fn} = 0$,   (7-9)

where, in view of (7-6) and (7-7), the forces subscripted with wn_i ($i = 1$ or 2), at the endpoints of the wall wn_i, are functions of the motions of nodes $(n-1)_i$ and n_i, and the forces subscripted fn at the floor are functions of the motions of nodes n_1 and n_2 (Figure 2). Equations (7-8) and (7-9) encode the exact discrete expression of the balance of the structure.

7D. *Expansions of the nodal forces.* The scale separation implies that at the frequency of an homogenizable mode, the own wavelength of each beam is much larger than its length, and therefore $\ell/\ell_T \ll 1$ and $\ell/\ell_L \ll 1$. It follows that the forces can then be developed according to the powers of $\ell_T^* = \ell/\ell_T$ and $\ell_L^* = \ell/\ell_L$, giving

$$
N(u_1, u_2) = \frac{EA}{\ell} \left(u_1 - u_2 - \frac{2u_1 + u_2}{6} \ell_L^{*2} - \frac{8u_1 + 7u_2}{360} \ell_L^{*4} + O(\ell_L^{*6}) \right),
$$

$$
T(v_1, v_2, \theta_1, \theta_2) = \frac{6EI_b}{\ell^3} \left(2(v_1 - v_2) + \ell(\theta_1 + \theta_2) - \frac{156v_1 + 54v_2 + \ell(22\theta_1 - 13\theta_2)}{2520} \ell_T^{*4} + O(\ell_T^{*8}) \right),
$$

$$
M(v_1, v_2, \theta_1, \theta_2) = \frac{2EI_b}{\ell^2} \left(3(v_1 - v_2) + \ell(2\theta_1 + \theta_2) - \frac{22v_1 + 13v_2 + \ell(4\theta_1 - 3\theta_2)}{840} \ell_T^{*4} + O(\ell_T^{*8}) \right).
$$

7E. *Balance equations for transverse vibrations.* In this case, the discrete variables $U(n)$, $\alpha(n)$, $\theta(n)$ are governed by the discrete balance equations (3-3):

$$\text{T}^E_{wn_1} + \text{T}^E_{wn_2} - \left(\text{T}^B_{w(n+1)_1} + \text{T}^B_{w(n+1)_2}\right) - (\text{N}^B_{fn} - \text{N}^E_{fn}) = 0,$$
$$\text{N}^E_{wn_2} - \text{N}^E_{wn_1} - \left(\text{N}^B_{w(n+1)_2} - \text{N}^B_{w(n+1)_1}\right) - (\text{T}^E_{fn} - \text{T}^B_{fn}) = 0,　　　　(7\text{-}10)$$
$$\text{M}^E_{wn_1} + \text{M}^E_{wn_2} - \left(\text{M}^B_{w(n+1)_1} + \text{M}^B_{w(n+1)_2}\right) - (\text{M}^B_{fn} - \text{M}^E_{fn}) = 0.$$

We now substitute the expansions for these quantities. For the case treated in the next section, it is sufficient to take terms up to order $(\ell/\ell_T)^8 \sim \omega^4$ and $(\ell/\ell_L)^4 \sim \omega^4$. We obtain for the balance in the transverse direction

$$\frac{24 E_w I_w}{\ell_w^2}\left(\frac{U_{(n+1)} - 2\,U_n + U_{(n-1)}}{\ell_w^2}\left[1 + \frac{3}{280}\left(\frac{\ell_w}{\ell_{Tw}}\right)^4\right] + \frac{\theta_{(n+1)} - \theta_{(n-1)}}{4\,\ell_w}\left[1 + \frac{13}{2520}\left(\frac{\ell_w}{\ell_{Tw}}\right)^4\right]\right.$$
$$\left. + \frac{U_n}{12}\left[\left(\frac{\ell_w}{\ell_{Tw}}\right)^4 + \frac{\ell_w}{\ell_f}\frac{E_f}{E_w}\frac{A_f\ell_w^2}{2\,I_w}\left(\frac{\ell_f}{\ell_{Lf}}\right)^2\right]\right) = O\left(\frac{\ell_w}{\ell_{Tw}}\right)^8 + O\left(\frac{\ell_f}{\ell_{Lf}}\right)^4. \quad (7\text{-}11)$$

Similarly, the other two balance equations become

$$\frac{E_w A_w \ell_f^2}{2}\left(\frac{\alpha_{(n+1)} - 2\,\alpha_n + \alpha_{(n-1)}}{\ell_w^2}\left[1 + \frac{1}{6}\left(\frac{\ell_w}{\ell_{Lw}}\right)^2\right] + \frac{\alpha_n}{\ell_w^2}\left(\frac{\ell_w}{\ell_{Lw}}\right)^2\right)$$
$$+ \frac{12\,E_f I_f}{\ell_w \ell_f}\left(\theta_n - \alpha_n - \frac{3\,\theta_n - 17\,\alpha_n}{1680}\left(\frac{\ell_f}{\ell_{Tf}}\right)^4\right) = O\left(\frac{\ell_f}{\ell_{Tf}}\right)^8 + O\left(\frac{\ell_w}{\ell_{Lw}}\right)^4,$$

$$\frac{24\,E_w I_w}{\ell_w^2}\left(\frac{U_{(n+1)} - U_{(n-1)}}{2\,\ell_w}\left[1 + \frac{13}{2520}\left(\frac{\ell_w}{\ell_{Tw}}\right)^4\right] + \frac{\theta_{(n+1)} - 2\,\theta_n + \theta_{(n-1)}}{6}\left[1 + \frac{1}{280}\left(\frac{\ell_w}{\ell_{Tw}}\right)^4\right]\right.$$
$$\left. + \theta_n\left[1 - \frac{1}{2520}\left(\frac{\ell_w}{\ell_{Tw}}\right)^4\right]\right) + \frac{12\,E_f I_f}{\ell_w \ell_f}\left[\theta_n - \alpha_n + \frac{2\,\theta_n - 9\,\alpha_n}{2520}\left(\frac{\ell_f}{\ell_{Tf}}\right)^4\right] = O\left(\frac{\ell_f}{\ell_{Tf}}\right)^8 + O\left(\frac{\ell_w}{\ell_{Tw}}\right)^8.$$

These equations may be modified in two steps. First we use the angular frequency ω_r of (3-4), to obtain (with $i = f, w$)

$$\left(\frac{\ell_i}{\ell_{Ti}}\right)^4 = \left(\frac{\ell_i}{L}\right)^2 \frac{2\,E_w A_w \ell_i^2}{E_i I_i}\frac{\lambda_i}{\Lambda}\left(\frac{\omega}{\omega_r}\right)^2, \qquad \left(\frac{\ell_i}{\ell_{Li}}\right)^2 = \left(\frac{\ell_i}{L}\right)^2 \frac{2\,E_w A_w}{E_i A_i}\frac{\lambda_i}{\Lambda}\left(\frac{\omega}{\omega_r}\right)^2. \quad (7\text{-}12)$$

We then introduce the continuous variables and their Taylor expansions. For instance,

$$\frac{U_{(n+1)} - 2\,U_n + U_{(n-1)}}{\ell_w^2} = U''(x) + O(\varepsilon^2 U''''(x)).$$

7F. *Slender-Timoshenko beam.* We now narrow the analysis to the case

$$E_f/E_w = O(1), \quad \rho_f/\rho_w = O(1), \quad \ell_f/\ell_w = O(1), \quad a_w/\ell_w = O(\varepsilon), \quad a_f/\ell_w = O(\varepsilon),$$

so

$$O\left(\frac{\ell_w}{\ell_{Tw}}\right)^4 = O\left(\frac{\ell_f}{\ell_{Tf}}\right)^4 = O\left(\frac{\omega}{\omega_r}\right)^2, \qquad O\left(\frac{\ell_w}{\ell_{Lw}}\right)^2 = O\left(\frac{\ell_f}{\ell_{Lf}}\right)^2 = \varepsilon^2 O\left(\frac{\omega}{\omega_r}\right)^2. \quad (7\text{-}13)$$

The transverse modes are attained when the inertia induced by the transverse motions is balanced by the transverse elastic forces. Therefore, focusing on the balance in the transverse direction (7-11), and

retaining the leading terms in the continuous representation, we get

$$\frac{2E_w I_w}{\ell_w^2}\left(12(U'' + \theta') + \frac{A_w \ell_w^2}{I_w}\frac{U}{L^2}\left(\frac{\omega}{\omega_r}\right)^2\right) = O\left(\frac{E_w I_w}{\ell_w^2}\left(\frac{\omega}{\omega_r}\right)^4 U''\right). \tag{7-14}$$

Since $U'' = O(U/L^2)$ and, in the slender-Timoshenko case under consideration, $A_w \ell_w^2/I_w = O(\varepsilon^{-2})$, the term $12(U'' + \theta')$ on the left-hand side of (7-14) (the elastic force) will be of the same order as the term following it (the inertia force) provided that

$$\omega/\omega_r = O(\varepsilon), \qquad \text{that is,} \qquad \omega = \tilde{\omega}_1.$$

This estimate enables us to write the expansions in powers of ε only. In the case under consideration, the leading orders of the three balance equations become

$$\frac{24E_w I_w}{\ell_w^2}\left(\tilde{U}^{0''} + \tilde{\theta}^{0'}\right) + \Lambda\tilde{\omega}_1^2\, \tilde{U}^0 = 0,$$

$$\frac{E_w A_w \ell_f^2}{2}\tilde{\alpha}^{0''} + \frac{12\, E_f I_f}{\ell_w \ell_f}(\tilde{\theta}^0 - \tilde{\alpha}^0) = 0, \tag{7-15}$$

$$\frac{24\, E_w I_w}{\ell_w^2}\left(\tilde{U}^{0'} + \tilde{\theta}^0\right) + \frac{12\, E_f I_f}{\ell_w \ell_f}(\tilde{\theta}^0 - \tilde{\alpha}^0) = 0.$$

This achieves zero order homogenization and leads to (4-6).

8. Conclusion

An application of HPDM is presented for dynamics of one-dimensional structures. Associated with a systematic use of scaling, the method provides four types of equivalent beam depending on the order of magnitude of the geometrical (then mechanical) characteristics of the cell. A generic beam of the sixth degree is shown to include all the mechanisms under transverse motions.

It is shown that, more than by the actual frame cell geometry, the macro behavior is governed by the three global cell parameters involved in the shear, global and inner bending constitutive beam laws. Then, expressed with those parameters, the beam-like descriptions may apply to other symmetric cells. The same principle could also be used for compression modes [Boutin and Hans 2003] and for twisting modes, not developed here.

Based on modal dimensional analysis, simple criteria of practical interest enable to identify the proper model for real structures, and to realize an easy, computer time efficient, analysis of the behavior. This approach provides large simplification for determining low frequency modes of discrete structures made of N cells. Provided that the dynamic excitation of the basis respects the scale separation, more precisely when its spectrum content does not exceed the frequency of the $(N/3)$-th mode, the complete dynamic calculation may be replaced by

(1) the calculation of the macroscopic parameters of a single cell submitted to a static strain, and

(2) the solving of the one-dimensional problem with the identified parameters, using either the generic beam model or the adequate specific beam.

The fact that in the specific case 5C the zero order description is valid up to the second order may explain the satisfactory accuracy of the beam modeling despite the weak scale separation.

Lastly, analogy with micromorphic media provides criteria to identify the nature of the effective behavior of discrete media. This latter may vary from Cauchy to complex micromorphic behavior according to the intrinsic parameters of the cell and the dimensions of the shearing zone.

The adaptability of the method enables extensions of this work from the field of structural dynamics to that of mechanics of heterogeneous materials. Recent experiments on regular buildings have demonstrated the reliability of this approach to describe the dynamics under shock, forced and ambient vibrations in term of a few first eigenmodes [Boutin et al. 2005]. Applications in biomechanics may also be envisaged.

Acknowledgements

References

[Bakhvalov and Panasenko 1989] N. Bakhvalov and G. Panasenko, *Homogenisation: averaging processes in periodic media: mathematical problems in the mechanics of composite materials*, Mathematics and its Applications (Soviet Series) **36**, Kluwer, Dordrecht, 1989.

[Bensoussan et al. 1978] A. Bensoussan, J.-L. Lions, and G. Papanicolaou, *Asymptotic analysis for periodic structures*, Studies in Mathematics and its Applications **5**, North-Holland, Amsterdam, 1978.

[Boutin 1995] C. Boutin, "Microstructural influence on heat conduction", *Int. J. Heat Mass Transf.* **38**:17 (1995), 3181–3195.

[Boutin and Auriault 1990] C. Boutin and J. L. Auriault, "Dynamic behaviour of porous media saturated by a viscoelastic fluid: application to bituminous concretes", *Int. J. Eng. Sci.* **28**:11 (1990), 1157–1181.

[Boutin and Auriault 1993] C. Boutin and J. L. Auriault, "Rayleigh scattering in elastic composite materials", *Int. J. Eng. Sci.* **31**:12 (1993), 1669–1689.

[Boutin and Hans 2003] C. Boutin and S. Hans, "Homogenisation of periodic discrete medium: application to dynamics of framed structures", *Comput. Geotech.* **30**:4 (2003), 303–320.

[Boutin et al. 2005] C. Boutin, S. Hans, E. Ibraim, and P. Roussillon, "*In situ* experiments and seismic analysis of existing buildings, II: Seismic integrity threshold", *Earthquake Eng. Struct. Dyn.* **34**:12 (2005), 1531–1546.

[Buannic and Cartraud 2001a] N. Buannic and P. Cartraud, "Higher-order effective modeling of periodic heterogeneous beams, I: Asymptotic expansion method", *Int. J. Solids Struct.* **38**:40-41 (2001), 7139–7161.

[Buannic and Cartraud 2001b] N. Buannic and P. Cartraud, "Higher-order effective modeling of periodic heterogeneous beams, II: Derivation of the proper boundary conditions for the interior asymptotic solution", *Int. J. Solids Struct.* **38**:40-41 (2001), 7163–7180.

[Caillerie et al. 1989] D. Caillerie, P. Trompette, and P. Verna, "Homogenisation of periodic trusses", pp. 7139–7180 in *10 years of progress in shell and spatial structures* (Madrid, 1989), CEDEX-Laboratorio Central de Estructuras y Materiales, Madrid, 1989.

[Cioranescu and Saint Jean Paulin 1999] D. Cioranescu and J. Saint Jean Paulin, *Homogenization of reticulated structures*, Applied Mathematical Sciences **136**, Springer, New York, 1999.

[Eringen 1968] A. C. Eringen, "Mechanics of micromorphic continua", pp. 18–35 in *IUTAM symposium on the generalized Cosserat continuum and the continuum theory of dislocations with applications*, Springer, Berlin, 1968.

[Gambin and Kröner 1989] B. Gambin and E. Kröner, "Higher-order terms in the homogenized stress-strain relation of periodic elastic media", *Phys. Status Solidi B* **151**:2 (1989), 513–519.

[Kerr and Accorsi 1985] A. D. Kerr and M. L. Accorsi, "Generalization of the equations for frame-type structures: a variational approach", *Acta Mech.* **56**:1-2 (1985), 55–73.

[Le Corre et al. 2004] S. Le Corre, D. Caillerie, L. Orgéas, and D. Favier, "Behavior of a net of fibers linked by viscous interactions: theory and mechanical properties", *J. Mech. Phys. Solids* **52**:2 (2004), 395–421.

[Mead 1996] D. M. Mead, "Wave propagation in continuous periodic structures: research contributions from Southampton 1964–1995", *J. Sound Vib.* **190**:3 (1996), 495–524.

[Moreau and Caillerie 1998] G. Moreau and D. Caillerie, "Continuum modeling of lattice structures in large displacement applications to buckling analysis", *Comput. Struct.* **68**:1-3 (1998), 181–189.

[Noor 1988] A. K. Noor, "Continuum modeling for repetitive lattice structures", *Appl. Mech. Rev.* (*ASME*) **41**:7 (1988), 285–296.

[Pradel and Sab 1998] F. Pradel and K. Sab, "Cosserat modelling of elastic periodic lattice structures", *C. R. Acad. Sci. II B Mec.* **326**:11 (1998), 699–704.

[Renton 1984] J. D. Renton, "The beam-like behavior of space trusses", *AIAA J.* **22**:2 (1984), 273–280.

[Sánchez-Palencia 1980] E. Sánchez-Palencia, *Non-homogeneous media and vibration theory*, Lecture Notes in Physics **127**, Springer, Berlin, 1980.

[Stephen 1999] N. G. Stephen, "On the vibration of one-dimensional periodic structures", *J. Sound Vib.* **227**:5 (1999), 1133–1142.

[Tollenaere 1994] H. Tollenaere, *Modèles bidimensionnels de tissés: homogénéisation des treillis en vibrations libres*, thèse de doctorat, Institut National Polytechnique de Grenoble, Grenoble, 1994.

[Tollenaere and Caillerie 1998] H. Tollenaere and D. Caillerie, "Continuum modeling of lattice structures by homogenization", *Adv. Eng. Software* **29**:7-9 (1998), 699–705.

[Trabucho and Viaño 1996] L. Trabucho and J. M. Viaño, "Mathematical modelling of rods", pp. 487–974 in *Handbook of numerical analysis*, vol. IV, edited by P. G. Ciarlet and J. L. Lions, North-Holland, Amsterdam, 1996.

[Verna 1991] P. Verna, *Modélisation continue des structures discrètes par homogénéisation: cas des treillis*, thèse de doctorat, Institut National Polytechnique de Grenoble, Grenoble, 1991.

STEPHANE HANS: stephane.hans@entpe.fr
École Nationale des Travaux Publics de l'État - Université de Lyon, Département Génie Civil et Bâtiment - URA CNRS 1652, rue Maurice Audin, 69518 Vaulx-en-Velin, France

CLAUDE BOUTIN: claude.boutin@entpe.fr
École Nationale des Travaux Publics de l'État - Université de Lyon, Département Génie Civil et Bâtiment - URA CNRS 1652, rue Maurice Audin, 69518 Vaulx-en-Velin, France